Molecular Phylogenetics and Evolution 154 (2021) 106962

Contents lists available at ScienceDirect

Molecular Phylogenetics and Evolution

journal homepage: www.elsevier.com/locate/ympev

Systematics of a Neotropical clade of dead-leaf-foraging antwrens (Aves: Thamnophilidae; *Epinecrophylla*)

Oscar Johnson*, Jeffrey T. Howard[1], Robb T. Brumfield

Department of Biological Sciences and Museum of Natural Science, Louisiana State University, Baton Rouge, LA 70803, USA

ARTICLE INFO

Keywords:
Systematics
Ultraconserved elements
Phylogenomics
Epinecrophylla
Amazonia

ABSTRACT

The stipple-throated antwrens of the genus *Epinecrophylla* (Aves: Thamnophilidae) are represented by eight species primarily found in the lowlands of the Amazon Basin and the Guiana Shield. The genus has a long and convoluted taxonomic history, with many attempts made to address the taxonomy and systematics of the group. Here we employ massively parallel sequencing of thousands of ultraconserved elements (UCEs) to provide both the most comprehensive subspecies-level phylogeny of *Epinecrophylla* antwrens and the first population-level genetic analyses for most species in the genus. Most of our results are robust to a diversity of phylogenetic and population genetic methods, but we show that even with thousands of loci we are unable to fully resolve the relationships between some western Amazonian species in the *haematonota* group. We uncovered phylogenetic relationships between taxa and patterns of population structure that are discordant with both morphology and current taxonomy. For example, we found deep genetic breaks between taxa in the *ornata* group that are currently regarded as species, and in the *haematonota* and *leucophthalma* groups we found paraphyly at the species and subspecies levels, respectively. As has been found in many Amazonian taxa, our phylogenetic results show that the major river systems of the Amazon Basin appear to have an effect on the genetic structure and range limits within *Epinecrophylla*. Our population genetics analyses showed extensive admixture between some taxa despite their deep genetic divergence. We present a revised taxonomy for the group and suggest areas for further study.

1. Introduction

The stipple-throated antwrens of the genus *Epinecrophylla* (Isler et al., 2006; Aves: Thamnophilidae) are represented by 21 currently recognized taxa, eight of which are considered species (*E. fulviventris*, *E. ornata*, *E. erythrura*, *E. leucophthalma*, *E. gutturalis*, *E. amazonica*, *E. spodionota*, and *E. haematonota*). These species are primarily found in the lowlands of the Amazon Basin and the Guiana Shield, with one (*E. fulviventris*) found west of the Andes from Ecuador to Honduras (Clements et al., 2019; Zimmer and Isler, 2003). All species are small, insectivorous dead-leaf foraging specialists, typically found in pairs or small family groups in tropical upland forest, and regularly attending mixed-species flocks (Remsen and Parker, 1984; Rosenberg, 1997; Wiley, 1971). The genus reaches its greatest diversity in the western Amazon Basin, with up to three species broadly co-occurring in most regions, despite similar plumage and foraging behavior between species (Remsen and Parker, 1984; Rosenberg, 1997; Zimmer and Isler, 2003).

Multiple attempts have been made to resolve relationships in the genus with molecular data, with increasing numbers of loci and individuals used (Hackett and Rosenberg, 1990; Harvey et al., in review; Whitney et al., 2013). Long considered to be in the genus *Myrmotherula*, early molecular work using protein electrophoresis provided the first indication that the stipple-throated antwren complex was not a close relative of other *Myrmotherula* antwrens (Hackett and Rosenberg, 1990). This was further supported with Sanger sequencing of mitochondrial and nuclear loci (Bravo et al., 2014; Brumfield et al., 2007; Irestedt et al., 2004), with these studies finding that *Epinecrophylla* was most closely related to bushbirds in the genera *Neoctantes* and *Clytoctantes*. This work led to the naming of a new genus for the group, *Epinecrophylla* (Isler et al., 2006), with *E. haematonota* as the type species. Some authorities changed the English common names of the *Epinecrophylla* species from antwrens to stipplethroats (Clements et al., 2019; Remsen et al., 2019) to reflect this taxonomic rearrangement.

* Corresponding author.
E-mail addresses: ojohns7@lsu.edu (O. Johnson), robb@lsu.edu (R.T. Brumfield).
[1] Present address: Louisiana State University Health Sciences Center Shreveport, Shreveport, LA 71103, USA.

https://doi.org/10.1016/j.ympev.2020.106962
Received 26 March 2020; Received in revised form 19 August 2020; Accepted 10 September 2020
Available online 18 September 2020

1.1. Taxonomic history

The species-level taxonomy of the genus has undergone considerable rearrangement through history (Cory and Hellmayr, 1924; Isler and Whitney, 2018; Peters, 1951; Whitney et al., 2013; Zimmer, 1932a; 1932b), particularly in the *haematonota* and *leucophthalma* groups. Early authors (e.g. Cory and Hellmayr, 1924) considered *E. haematonota* to include as subspecies the taxa *pyrrhonota* and *amazonica* and placed both *spodionota* and *sororia* as subspecies of *E. leucophthalma*, largely based on back color (rufous in the former three taxa, brown in the latter three). Using this same reasoning, Todd (1927), when describing the rufous-backed form *phaeonota* treated it as a subspecies of *E. haematonota*, but incongruously considered the rufous-backed *E. amazonica* a species distinct from all other forms. Zimmer (1932a), however, noted that back color may not be a valid species-level character and citing other morphological characters (primarily the shape of the pale spots on the wing coverts) transferred *amazonica, spodionota*, and *sororia* to *E. haematonota*, and *phaeonota* to *E. leucophthalma*. Zimmer (1932a) suggested the possibility of species rank for the rufous-backed taxon *phaeonota*, but also noted intermediate individuals between it and the adjacent brown-backed taxa *leucophthalma* and *sordida*. This treatment was maintained by most authors (e.g. Meyer de Schauensee, 1970; Peters, 1951) until Parker and Remsen (1987) recognized *E. spodionota* (including *sororia*) of the Andean foothills as a separate species. This taxonomic treatment was augmented by the recent discovery of two range-restricted taxa in the group, each described as a new species; *E. fjeldsaai* of eastern Ecuador and far northern Peru (Krabbe et al., 1999), and *E. dentei* of the Aripuanã-Machado region of Brazil (Whitney et al., 2013). In describing *E. dentei*, Whitney et al. (2013) also estimated a mitochondrial phylogeny of the genus, including samples of most taxa, in which they found *fjeldsaai* was phylogenetically embedded within *haematonota*. Based on the work of Whitney et al. (2013) and the mitochondrial distances between taxa, Remsen et al. (2019) separated *E. haematonota* into four species: *E. fjeldsaai* (based on morphological differences), *E. pyrrhonota*, *E. haematonota*, and *E. amazonica* (including *dentei*), whereas other authors united *pyrrhonota*, *amazonica*, and *dentei* under *E. haematonota* while maintaining *E. fjeldsaai* as a distinct species (Dickinson and Christidis, 2014). Since then, Isler and Whitney (2018) conducted a thorough analysis of the vocalizations of *haematonota*, *fjeldsaai*, and *pyrrhonota* in which they found no vocal differences among the three taxa, leading to the recognition of the latter two taxa as subspecies of the former (Remsen et al., 2019).

Within *E. ornata*, the gray-backed Peruvian taxon *atrogularis* was long considered a separate species, leaving the rufous-backed forms *saturata* and *hoffmannsi* as subspecies of *E. ornata* (Cory and Hellmayr, 1924). This treatment was maintained until Zimmer (1932b) described the gray-backed *meridionalis* as a subspecies and united all five taxa in the group under the species *E. ornata*. This is the current treatment of most recent authors (Clements et al., 2019; Dickinson and Christidis, 2014; Remsen et al., 2019), although del Hoyo et al. (2019) consider *E. hoffmannsi* a species separate from the rest of *E. ornata* based primarily on the unique female plumage and minor vocal differences.

The taxonomy of the remainder of the genus has remained rather more stable through time, with the three other species – *E. fulviventris*, *E. gutturalis,* and *E. erythrura* – all largely considered independent species by most authors. *E. erythrura* and *E. leucophthalma* are currently considered polytypic, while the four taxa described in *E. fulviventris* are generally considered synonyms of the nominate subspecies (Cory and Hellmayr, 1924; Zimmer and Isler, 2003).

Much of the previous molecular phylogenetic work in *Epinecrophylla* has relied upon mitochondrial sequence data, although a recent phylogenomic study of all suboscine passerine birds using sequence capture of ultraconserved elements (UCEs) included 1–2 samples of each species of *Epinecrophylla* and recovered a well-resolved topology for the genus (Harvey et al., in review). Here we expand on the previous genetic work in the genus, addressing the systematics of the group with population-level sampling of most taxa, and both next-generation sequencing of thousands of nuclear loci and draft mitochondrial genomes. We follow the taxonomy of the South American Classification Committee (Remsen et al., 2019) and make taxonomic recommendations in light of the Biological Species Concept (Mayr, 1942) in its modern form, namely that "species are groups of interbreeding natural populations that are reproductively isolated from other such groups" (de Queiroz, 2007; Mayr, 1996). We opt for a genetic yardstick approach in this study due to our lack of morphological data or detailed studies of potential hybrid zones in the group. We use genetic distances and the presence or absence of admixed genotypes of known species (assessed via lack of interbreeding in sympatry) to assess the species status of allopatric taxa. *Epinecrophylla* provide a unique system in which to study speciation in the Amazon Basin due to their high species diversity, documented phenotypic hybrid zones, and multiple broadly sympatric species. Our expanded sampling both of individuals and loci provides the most in-depth view of the evolutionary history, species limits, population structure, and introgression between taxa in this group.

2. Methods

2.1. Sampling

We obtained a total of 66 *Epinecrophylla* representing 18 of the 21 widely recognized taxa in the genus and all currently recognized species. Missing ingroup taxa are *E. o. ornata*, *E. o. saturata*, and *E. leucophthalma dissita*. The three outgroup species we used are *Myrmorchilus strigilatus*, *Neoctantes niger*, and *Clytoctantes atrogularis*. When available, we obtained samples from across the geographic range of each *Epinecrophylla* taxon, with one sample chosen per geographic locality. Fifty-three tissue samples were obtained from vouchered specimens housed at museums in the United States, with sequence data for the remaining 16 samples obtained from Harvey et al. (in review; Table 1).

We extracted total DNA from the 53 tissue samples using ca. 25 mg of pectoral muscle with a Qiagen DNeasy Blood and Tissue Kit (Qiagen; Hilden, Germany) and quantified DNA concentration using a Qubit 2.0 fluorometer (Life Technologies Corporation; Carlsbad, CA). Samples were standardized to 10 ng/uL. We then sheared samples to approximately 600 base pair (bp) fragments with an Episonic 1100 bioprocessor (EpiGentek; Farmingdale, NY) and assessed fragment length using a High Sensitivity DNA Assay on an Agilent 2100 Bioanalyzer (Agilent Technologies; Santa Clara, CA). We generated DNA libraries using a KAPA Biosystems Hyper Prep kit (Wilmington, Massachusetts, USA) and enriched UCEs using a set of 5742 probes that target 5060 loci in vertebrates ("Tetrapods-UCE-5Kv1"; uce-5 k-probes.fasta) following the protocol of Faircloth et al. (2012). Enriched samples were pooled at equimolar ratios and paired-end sequencing was conducted on one lane of a HiSeq 3000 sequencer at Oklahoma Medical Research Foundation Clinical Genomics Center (OMRF; Oklahoma City, Oklahoma, USA). The sequencing lane contained DNA libraries used in other projects. The 16 samples obtained from Harvey et al. (in review) were enriched using a custom probe set consisting of 2500 vertebrate UCEs and 96 exons.

2.2. Contig assembly

OMRF demultiplexed sequence reads using custom scripts. We trimmed raw reads of adapter contamination and low-quality bases using illumiprocessor (Faircloth, 2013) and trimmomatic (Bolger et al., 2014) with default settings. We then subsampled all read files to 2 million reads per individual to decrease computation time for contig assembly and to normalize assemblies across samples. Read data were assembled with Itero (https://github.com/faircloth-lab/itero). Because samples were sequenced with two different probe sets, we opted to match contigs to the "Tetrapods-UCE-2.5Kv1" (uce-2.5 k-probes.fasta) probe set which consists of 2560 baits targeting 2386 UCE loci, and is a

Table 1
Localities for samples used in this project. Abbreviations are as follows: LSUMNS = Louisiana State University Museum of Natural Science, KU = University of Kansas Biodiversity Institute & Natural History Museum, AMNH = American Museum of Natural History, MZUSP = Museum of Zoology of the University of São Paulo, FMNH = Field Museum of Natural History, MSB = Museum of Southwestern Biology, USNM = Smithsonian National Museum of Natural History, YPM = Yale Peabody Museum. Accession numbers with the SAMN- prefix are the BioSample accession numbers for the samples sequenced for this project and deposited in the NCBI Sequence Read Archive (SRA) under BioProject number PRJNA622761. Accession numbers with other prefixes refer to NCBI GenBank mitochondrial gene sequences. Probe set refers to the probe set used in sequencing. 5 k = Tetrapods-UCE-5Kv1 probe set targeting 5060 loci, and sequenced for this study. 2.5 k = Tetrapods-UCE-2.5Kv1 probe set targeting 2386 loci, sequences obtained from Harvey et al. (in review).

Sample #	Taxon	Tissue #	Accession #	Probe set	Locality	Latitude	Longitude
1	*Epinecrophylla fulviventris*	LSUMNS 82086	SAMN14526248	5 k	Costa Rica: Limón; Reserva Biológica Hitoy-Cerere	9.65	−83.01
2	*E. fulviventris*	LSUMNS 2299	SAMN14526249; HM637244	2.5 k	Panamá: Darién; Cana	7.92	−77.70
3	*E. ornata atrogularis*	MSB 36505	SAMN14526250	5 k	Perú: San Martín; ca 2.7 km S of Plataforma	−7.41	−76.27
4	*E. ornata atrogularis*	LSUMNS 74213	SAMN14526251	2.5 k	Perú: Pasco; Provincia Oxapampa, Distrito Puerto Bermúdez, Comunidad San Juan	−10.50	−74.81
5	*E. ornata hoffmannsi*	LSUMNS 78113	SAMN14526252	2.5 k	Brazil: Amazonas; Barra de São Manuel	−7.50	−58.26
6	*E. ornata hoffmannsi*	FMNH 391379	SAMN14526253	5 k	Brazil: Pará; Serra dos Carajás	−6.28	−50.58
7	*E. ornata hoffmannsi*	FMNH 457051	SAMN14526254	5 k	Brazil: Pará; Portel, FLONA do Caxiuanã, Plot PPBIO	−2.53	−50.85
8	*E. ornata meridionalis*	LSUMNS 9502	SAMN14526255	5 k	Bolivia: Pando; Nicolás Suarez, 12 km by road S of Cobija, 8 km W on road to Mucden	−11.16	−68.78
9	*E. ornata meridionalis*	LSUMNS 1082	SAMN14526256	5 k	Bolivia: La Paz; Río Beni, ca 20 km by river N Puerto Linares	−15.28	−67.50
10	*E. ornata meridionalis*	LSUMNS 78808	SAMN14526257	5 k	Perú: Madre de Dios; Portillo, ca 7 km S Iberia	−11.45	−69.52
11	*E. erythrura erythrura*	ANSP 16560	SAMN14526258	2.5 k	Ecuador: Morona-Santiago; Santiago	−2.72	−78.32
12	*E. erythrura septentrionalis*	LSUMNS 27716	SAMN14526259	5 k	Perú: Loreto; 79 km WNW Contamana	−7.15	−75.69
13	*E. leucophthalma leucophthalma* west	LSUMNS 42670	SAMN14526260	5 k	Perú: Loreto; ca 54 km NNW mouth of Río Morona on W bank	−4.29	−77.24
14	*E. leucophthalma leucophthalma* west	LSUMNS 10538	SAMN14526261	5 k	Perú: Ucayali; W bank Río Shesha, 65 km ENE Pucallpa	−7.95	−74.25
15	*E. leucophthalma leucophthalma* west	LSUMNS 9173	SAMN14526262	5 k	Bolivia: Pando; Nicolás Suarez, 12 km by road S of Cobija, 8 km W on road to Mucden	−11.16	−68.78
16	*E. leucophthalma leucophthalma* west	LSUMNS 75006	SAMN14526263	5 k	Perú: Ucayali; Otorongo, 31.9 km ESE mouth of Río Cohengua	−10.38	−73.72
17	*E. leucophthalma sordida*	FMNH 392048	SAMN14526264	5 k	Brazil: Mato Grosso do Norte; Municipio Alta Floresta, upper Rio Teles Pires-Rio Cristalino	−9.63	−55.93
18	*E. leucophthalma sordida*	FMNH 457026	SAMN14526265	5 k	Brazil: Pará; Portel, FLONA do Caxiuanã, Plot PPBIO	−2.53	−50.85
19	*E. leucophthalma leucophthalma* east	FMNH 389907	SAMN14526266	5 k	Brazil: Rondônia; Cachoeira Nazaré, W bank Río Jiparaná	−10.36	−61.82
20	*E. leucophthalma leucophthalma* east	LSUMNS 36628	SAMN14526267	5 k	Brazil: Rondônia; Reserva Biológica Rebid Duro Preto, ca 70 km E Guajará-Mirim	−10.80	−64.69
21	*E. leucophthalma leucophthalma* east	LSUMNS 18242	SAMN14526268; HM637246	2.5 k	Bolivia: Santa Cruz; Provincia Velasco; PN Noel Kempff Mercado, 86 km ESE Florida	−14.85	−60.46
22	*E. leucophthalma leucophthalma* east	LSUMNS 14575	SAMN14526269	5 k	Bolivia: Santa Cruz; Serranía de Huanchaca, 21 km SE Catarata Arco Iris	−13.92	−60.82
23	*E. leucophthalma leucophthalma* east	LSUMNS 12394	SAMN14526270	5 k	Bolivia: Santa Cruz; Provincia Velasco, 32 km E Aserradero Moira, pre PN Noel Kempff Mercado	−14.60	−60.92
24	*E. leucophthalma phaeonota*	LSUMNS 85998	SAMN14526271	5 k	Brazil: Amazonas; Río Sucunduri	−6.89	−59.07
25	*E. leucophthalma phaeonota*	LSUMNS 78380	SAMN14526272	5 k	Brazil: Amazonas; Río Juruena	−11.05	−58.65
26	*E. leucophthalma phaeonota*	LSUMNS 77807	SAMN14526273	5 k	Brazil: Amazonas; Barra de São Manuel, W bank Río Tapajós	−7.34	−58.09
27	*E. leucophthalma phaeonota*	LSUMNS 80818	SAMN14526274	5 k	Brazil: Amazonas; right bank of Río Sucunduri, Igarapé da Cabaça	−5.70	−59.16
28	*E. leucophthalma phaeonota*	LSUMNS 35603	SAMN14526275	5 k	Brazil: Pará; ca 139 km WSW Santarém, W of Río Tapajós, Alto Río Arapiuns	−3.60	−55.52
29	*E. leucophthalma phaeonota*	LSUMNS 80774	SAMN14526276	5 k	Brazil: Amazonas; left bank of Río Sucunduri, left bank lower Río Acari (7 km from its mouth)	−7.15	−59.91
30	*E. gutturalis*	AMNH 12689	SAMN14526277	5 k	Venezuela: Amazonas; Cerro de La Neblina base camp	1.3	−66.5
31	*E. gutturalis*	YPM 139781	SAMN14526278	5 k	Suriname: upper West River Valley, Wilhelmina Mountains	3.75	−56.50
32	*E. gutturalis*	LSUMNS 71576	SAMN14526279	5 k	Suriname: Sipaliwini; Nassau Bebergte	4.78	−54.60
33	*E. gutturalis*	KU 88804	SAMN14526280	5 k	Guyana: Iwokrama Reserve, W bank Essequibo River, ca 72 river km SW Kurupukari	4.22	−59.17
34	*E. gutturalis*	KU 88801	SAMN14526281	5 k	Guyana: Iwokrama Reserve, ca 41 road km SW Kurupukari	4.34	−58.85
35	*E. gutturalis*	USNM 609157	SAMN14526282	5 k	Guyana: Essequibo Islands; West Demerara, Waruma River, E bank, ca 15 river km S Kako River	5.5	−60.6
36	*E. gutturalis*	USNM 586379	SAMN14526283	5 k	Guyana: Northwest District; Baramita	7.35	−60.35
37	*E. gutturalis*	AMNH 11921	SAMN14526284	5 k	Venezuela: Bolívar	6.2	−63.6
38	*E. gutturalis*	YPM 137211	SAMN14526285	5 k	Suriname: Sipaliwini; Werehpai	3.65	−56.20
39	*E. gutturalis*	LSUMNS 20398	SAMN14526286	2.5 k	Brazil: Amazonas; Manaus, km 34 ZF-3 Faz Esteio ca 80 km N Manaus	−2.44	−59.89
40	*E. gutturalis*	LSUMNS 55218	SAMN14526287; KC768924	2.5 k	Suriname: Sipaliwini; Balchuis Gebergte, ca 70 km SE Apura	4.73	−56.75
41	*E. gutturalis*	USNM 587338	SAMN14526288	5 k	Guyana: Acari Mountains, N side	2.05	−57.55
42	*E. gutturalis*	YPM 139633	SAMN14526289	5 k	Suriname: Para District	5.4	−55.2
43	*E. gutturalis*	YPM 101670	SAMN14526290	5 k	Suriname: Tafelberg	3.78	−56.15
44	*E. amazonica dentei*	MZUSP 80591	SAMN14526291; KC768944	2.5 k	Brazil: Amazonas; Río Roosevelt, Esperança	−8.33	−60.99
45	*E. amazonica amazonica*	LSUMNS 9217	SAMN14526292; KC768934	2.5 k	Bolivia: Pando; Nicolás Suarez, 12 km by road S of Cobija, 8 km W on road to Mucden	−11.20	−68.78
46	*E. amazonica amazonica*	MZUSP J164	SAMN14526293; KC768938	2.5 k	Brazil: Rondônia; left bank Río Madeira, near mouth of Río Abunã	−9.63	−65.45
47	*E. amazonica amazonica*	LSUMNS 31342	SAMN14526294	5 k	Brazil: Rondônia; ca 50 km NW Jaci Paraná, W bank of Río Madeira	−8.93	−64.10
48	*E. spodionota sororia*	KU 113634	SAMN14526295	5 k	Perú: Cusco; ca Alto Manguriari	−13.53	−71.97
49	*E. spodionota sororia*	LSUMNS 2058	SAMN14526296	5 k	Perú: Pasco; Puellas, km 41 on Villa Rica - Puerto Bermúdez highway	−10.29	−74.94
50	*E. spodionota sororia*	LSUMZ 76377	SAMN14526297	5 k	Perú: Ucayali; north ridge of Quebrada Quirapokiari watershed	−10.45	−74.12

(*continued on next page*)

Table 1 (*continued*)

Sample #	Taxon	Tissue #	Accession #	Probe set	Locality	Latitude	Longitude
51	*E. spodionota spodionota*	IAvH-BT 234	SAMN14526298	2.5 k	Colombia: Cauca; Santa Rosa, Serranía de Los Churumbelos, Río Alto Hornoyaco	1.70	−76.57
52	*E. spodionota sororia*	FMNH 474124	SAMN14526299	5 k	Perú: Amazonas; Río Verde	−6.72	−77.43
53	*E. spodionota sororia*	LSUMNS 5392	SAMN14526300	5 k	Perú: San Martín; 20 km by road NE Tarapoto on road to Yurimaguas	−6.36	−76.24
54	*E. haematonota pyrrhonota*	LSUMNS 4202	SAMN14526301; KC768931	2.5 k	Perú: Loreto; Lower Río Napo region, E bank Río Yanayacu, ca 90 km N Iquitos	−2.96	−73.24
55	*E. haematonota pyrrhonota*	FMNH 457014	SAMN14526302	5 k	Brazil: Amazonas; Maraã, Lago Cumapi	−1.68	−65.83
56	*E. haematonota pyrrhonota*	AMNH 14224	SAMN14526303	5 k	Brazil: Amazonas; Estrada Manacapuru-Novo Airão km 75	−3.29	−60.63
57	*E. haematonota pyrrhonota*	MZUSP 79027	SAMN14526304; KC768936	2.5 k	Brazil; Roraima; Paracaima, Comunidade Nova Esperança	4.43	−61.13
58	*E. haematonota pyrrhonota*	LSUMNS 7505	SAMN14526305	5 k	Venezuela: Amazonas; Cerro De La Neblina, Camp VII	0.88	−65.99
59	*E. haematonota haematonota*	LSUMNS 75291	SAMN14526306	5 k	Perú: Ucayali; Otorongo, 31.9 km ESE mouth of Río Cohengua	−10.38	−73.72
60	*E. haematonota haematonota*	LSUMNS 4579	SAMN14526307; HM449839	2.5 k	Perú: Loreto; S Río Amazonas, 10 km SSW mouth Río Napo on E bank Quebrada Vainilla	−3.52	−72.81
61	*E. haematonota haematonota*	LSUMNS 10790	SAMN14526308	5 k	Perú: Ucayali; W bank Río Shesha, 65 km ENE Pucallpa	−7.94	−74.23
62	*E. haematonota fjeldsaai* hybrid?	LSUMNS 42704	SAMN14526309	5 k	Perú: Loreto; ca 54 km NNW mouth of Morona on W bank	−4.29	−77.24
63	*E. haematonota fjeldsaai*	KU 873	SAMN14526310; KC768922	2.5 k	Perú: Loreto; San Jacinto, 1.5 km E Río Tigre	−2.32	−75.86
64	*E. haematonota haematonota*	LSUMNS 93087	SAMN14526311	5 k	Perú: Loreto; Esperanza, E of Río Huallaga on Río Yuracyacu, 14.2 km E Santa Cruz	−5.54	−75.73
65	*E. haematonota haematonota*	LSUMNS 27427	SAMN14526312	5 k	Perú: Loreto; NE bank upper Río Cushabatay, 84 km WNW Contamana	−7.07	−75.70
66	*E. haematonota haematonota*	LSUMNS 42282	SAMN14526313	5 k	Perú: Loreto; 7 km SW Jeberos	−5.34	−76.32
outgroup	*Clytoctantes atrogularis*	MZUSP 96888	SAMN14526314	2.5 k	Brazil: Amazonas; Río Sucunduri (right bank) 60 km below BR-230 (point 9)	−6.25	−59.07
outgroup	*Myrmorchilus strigilatus*	LSUMNS 18722	SAMN14526315	5 k	Bolivia: Santa Cruz; Provincia Cordillera, Estancia Perforación, ca 130 km E Charagua	−19.78	−61.97
outgroup	*Neoctantes niger*	LSUMNS 2749	SAMN14526316	2.5 k	Perú: Loreto; 1 km N Río Napo, 157 km by river NNE Iquitos	−3.39	−73.18

subset of the other probe sets used in sequencing. For the samples sequenced with the "Tetrapods-UCE-5Kv1" probe set, we separately matched assembled contigs to this probe set.

2.3. Sample identification and locus filtering

To confirm the identifications of samples we used the Phyluce 1.6.7 (Faircloth, 2015) tool *match_contigs_to_barcodes* to match contigs from each sample to a mitochondrial Cytochrome *c* oxidase subunit I (COI) barcode sequence of *Epinecrophylla pyrrhonota* obtained from GenBank (JN801852.1) and map those contigs against the Barcode of Life Database (BOLD; Ratnasingham and Hebert, 2007). We then used the Phyluce 1.6.7 (Faircloth, 2015) tool *get_trinity_coverage* to calculate per-locus read coverage for all contigs matching either UCE and mitochondrial loci. Three samples contained mitochondrial loci with high coverage (> 30x) that matched the incorrect species in BOLD, suggesting either sample misidentification or high levels of contamination, and were eliminated from our dataset (Table S1). Nine additional samples contained high-coverage mitochondrial contigs matching the expected species in BOLD, but with a small number of low-coverage mitochondrial contigs matching the incorrect species. We used the maximum coverage of 8.05x of these potentially contaminated low-coverage mitochondrial contigs as a filter and removed all UCE contigs across all samples that had an average read depth below this threshold.

2.4. Mitochondrial genome assembly

We used off-target reads from the UCE sequencing to assemble draft mitochondrial genomes. We assembled mitochondrial genomes in MITObim 1.9 (Hahn et al., 2013), which is a Perl wrapper for MIRA 4.0.2 (Chevreux et al., 1999), using as a reference the complete mitochondrial genome of *Myrmoderus loricatus* (G. Bravo, unpublished data) and the *–quick* option. We annotated the assembled mitochondrial genomes using the MITOchondrial genome annotation Server (MITOS) 2 (Bernt et al., 2013) and aligned the 13 mitochondrial protein coding genes in MAFFT (Katoh et al., 2002) implemented in Geneious 10.2.3 (https://www.geneious.com) to create a final partitioned draft mitogenome alignment.

2.5. Nuclear locus phasing, alignment, and SNP calling

To phase UCE loci we selected as a reference the individual from our sampling that contained the greatest number of UCE loci after filtering; *Epinecrophylla leucophthalma* LSUMNS 42670. We phased UCE loci using the *seqcap_pop* pipeline (https://github.com/mgharvey/seqcap_pop; Faircloth, 2015; Harvey et al., 2016) to obtain a Single Nucleotide Polymorphism (SNP) dataset and followed Andermann et al. (2019) to obtain phased alignments. The *seqcap_pop* pipeline utilizes tools from the Phyluce package (Faircloth, 2015), SAMtools 0.1.19 (Li et al., 2009), Picard (Broad Institute, Cambridge, MA), BWA 0.7.17 (Li and Durbin, 2009), and GATK 3.3.0 (McKenna et al., 2010) to process next-generation sequence data for population-level genetic analyses. Briefly, *seqcap_pop* maps sequencing reads to the reference individual to obtain a pileup, adds read groups and marks PCR duplicate reads for each individual, merges bam files within each species, calls indels and single-nucleotide polymorphisms on merged bam files, and phases high-quality indels and SNPs to produce vcf files of phased SNPs. We further filtered this dataset using vcftools 0.1.16 (Danecek et al., 2011) to remove SNPs with quality scores less than 30 and read depth less than 5.5, those with greater than 75% missing data, restricted to bi-allelic loci, and removed indels. We refer to this dataset as the "linked SNP dataset", as it contains multiple SNPs per locus. We then sampled at random one SNP per UCE locus to obtain a final dataset of putatively unlinked SNPs, which we refer to as the "unlinked SNP dataset". To obtain phased alignments we used Phyluce 1.6.7 (Faircloth, 2015) to phase UCE loci following Andermann et al. (2019), phasing data by

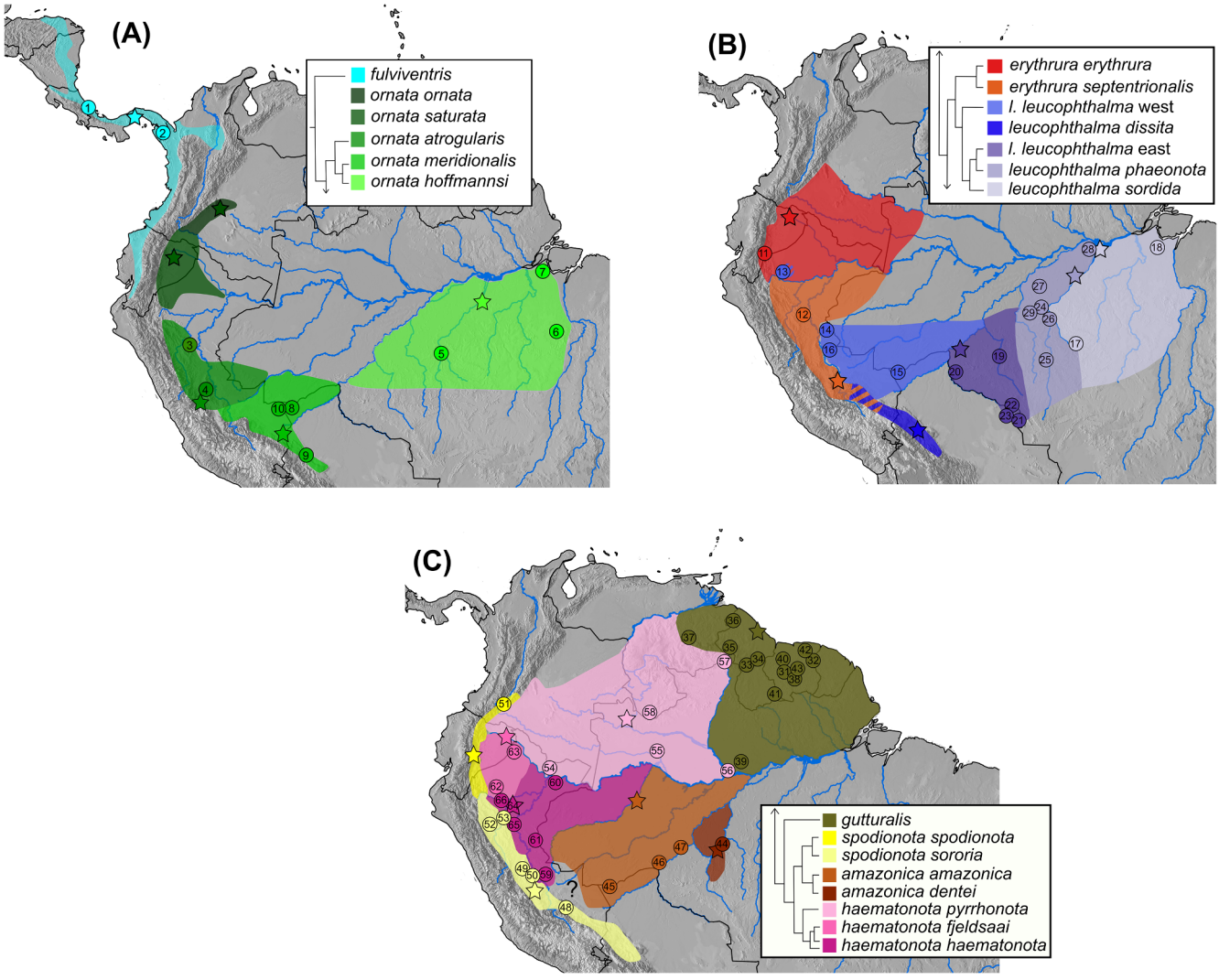

Fig. 1. Maps showing taxon distributions, type localities, and sample localities used in this study. A) *Epinecrophylla fulviventris* and *ornata*. B) *E. erythrura* and *leucophthalma*. C) *E. gutturalis, pyrrhonota, dentei, amazonica, spodionota, haematonota,* and *fjeldsaai*. Country boundaries are shown in black. Major rivers are shown in blue. Locations sampled for this study are indicated with a number, corresponding to sample information in Table 1. Type localities, shown with a star, are based on Peters (1951) or type descriptions. Hashed regions indicate range overlap. Inset for each map shows a cladogram of relationships between each taxon based on the trees in Fig. 2 and Fig S1A. The taxa that we were unable to sample in this study are included in the distribution maps and legend, but are not included in the reference cladogram. The species distributions illustrated here are based on published information (Clements et al., 2019; Cory and Hellmayr, 1924; del Hoyo et al., 2019; Dickinson and Christidis, 2014; Krabbe et al., 1999; Meyer de Schauensee, 1970; Peters, 1951; Schulenberg et al., 2007; Whitney et al., 2013; Zimmer 1932a, 1932b; Zimmer and Isler, 2003), museum specimen records (LSUMNS specimens and Marco Rego pers. comm.), photo-supported occurrence records in citizen science databases (eBird, WikiAves), and the genetic results presented here. (For interpretation of the references to color in this figure legend, the reader is referred to the web version of this article.)

mapping reads against the reference individual using the Phyluce tools *snp_bwa_align* and *snp_phase_uces*. This pipeline maps raw reads against contigs of a reference individual using BWA 0.7.17 (Li and Durbin, 2009), and then sorts and phases alleles in SAMtools 0.1.19 (Li and Durbin, 2009) and Picard (Broad Institute, Cambridge, MA). We used MAFFT 7.130b (Katoh and Standley, 2013) in the Phyluce tool *align_seqcap_align* to align and edge-trim the contigs output by this pipeline, treating the two alleles as separate individuals and allowing ambiguous sites in alignments. We produced a final alignment using the Phyluce 1.6.7 (Faircloth, 2015) tool *get_only_loci_with_min_taxa* to produce a 75% complete data matrix. This tool calculates the data matrix completeness as the percentage of individuals in the dataset with sequence data for each locus.

To investigate fine-scale patterns of population structure within each species we called SNPs within each species or species complex to obtain an additional six SNP datasets. We grouped samples based on the clades in the ExaBayes phylogeny estimated from the 75% complete UCE data matrix (see section 2.6 and Fig. 2). Three clades corresponded to species (*E. ornata*, *E. leucophthalma*, and *E. gutturalis*) and a fourth to a set of closely related taxa that have undergone considerable taxonomic rearrangement through history (*dentei*, *amazonica*, *spodionota*, *sororia*, *pyrrhonota*, *haematonota*, and *fjeldsaai*). This latter clade is hereafter referred to as the "*haematonota s.l.*" clade. Although *E. gutturalis* is part of the *haematonota s.l.* clade, we analyze the population genetic data separately due to the relatively deep genetic split of *E. gutturalis* from the rest of the clade. Within the *haematonota s.l.* clade we additionally subdivided taxa into two clades for SNP calling: one containing *dentei*, *amazonica*, *spodionota*, and *sororia* (hereafter the "*amazonica/spodionota*" clade), and the other containing *pyrrhonota*, *haematonota*, and *fjeldsaai* (hereafter the "*haematonota/pyrrhonota*" clade). For each dataset we selected as a reference the individual with the highest number of assembled contigs after filtering (Supplemental Table 4) and repeated the *seqcap_pop* pipeline described above.

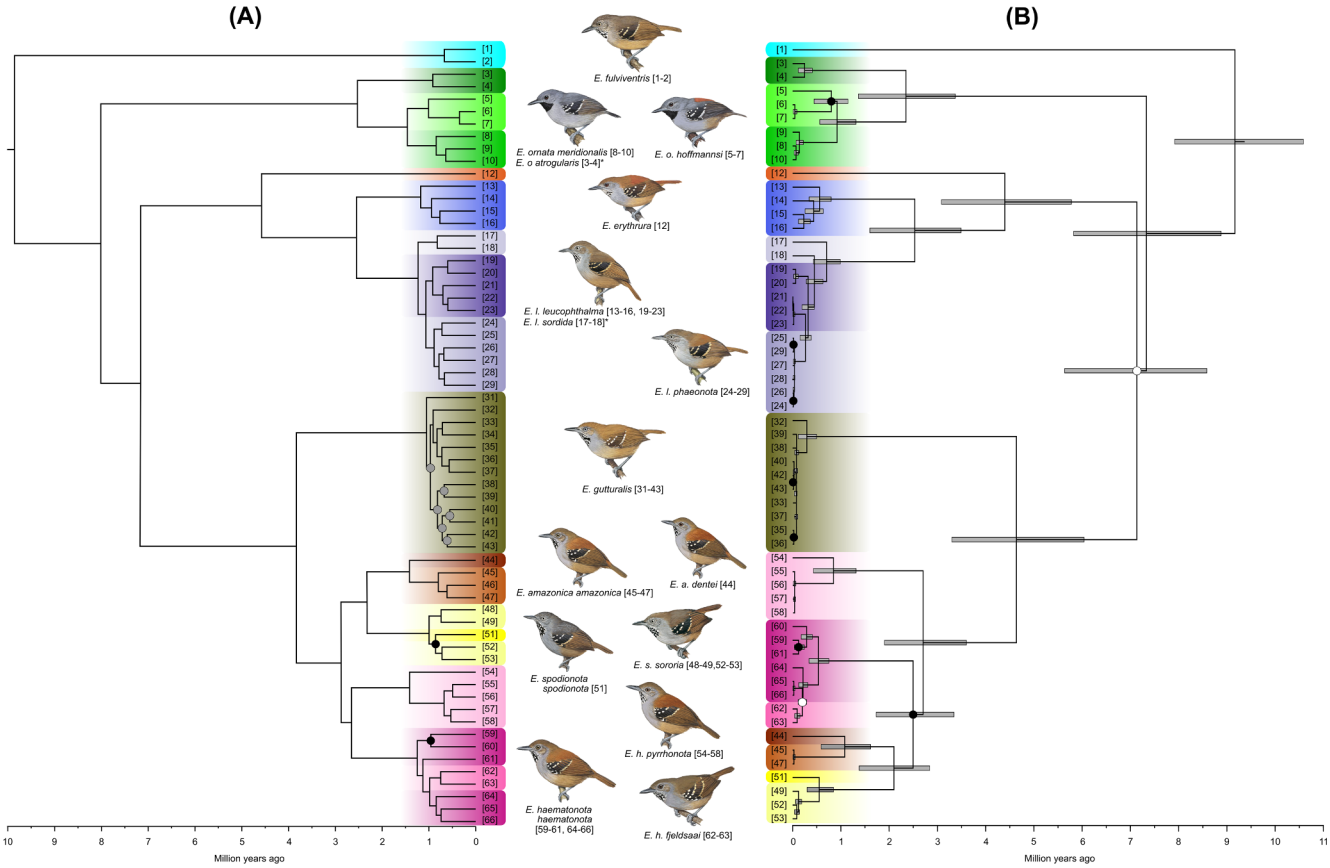

Fig. 2. Dated phylogenies estimated from UCE (A) and mitogenome (B) sequence data. A) Topology estimated in Exabayes from the 75% complete phased concatenated UCE data matrix and branch lengths optimized in treePL with date calibrations from Harvey et al. (in review). See section 2.6 for details. B) A dated phylogeny estimated from a partitioned analysis of the 13 mitochondrial protein-coding genes in BEAST 2.5.2 (Bouckaert et al., 2019), with nodes showing the 95% highest posterior density of the divergence estimates. Note that some samples did not contain sufficient mitochondrial data for analysis and are not included in this phylogeny. In both A and B, all nodes received full support unless marked with a circle. Nodes with a white circle with $>$ 0.50 posterior probability, nodes with a gray circle with $>$ 0.75 posterior probability, and nodes with a black circle with $>$ 0.90 posterior probability. Nodes in the mitochondrial phylogeny with a posterior probability $<$ 0.50 have been collapsed to a polytomy. Outgroup samples have been removed for clarity. Colors and sample numbers correspond to those in Fig. 1. Illustrations (all of males) reproduced by permission of Lynx Edicions. Taxa marked with an asterisk are not illustrated and are placed below the taxon they most closely resemble in plumage.

2.6. Phylogenetic estimation

From the 2386-locus UCE dataset we estimated a phylogenetic tree with all samples using a Bayesian analysis in ExaBayes 1.5 (Aberer et al., 2014) using the 75% complete concatenated phased alignment. We conducted 4 independent runs for 2 million generations each, discarding the first 25% of trees as burn-in. After checking in Tracer 1.7.1 (Rambaut et al., 2018) that samples had converged based on ESS values greater than 200, we generated an extended majority-rule consensus tree using the topologies from the four independent runs.

No fossils are available for *Epinecrophylla* or its close relatives to allow for a fossil calibration of our phylogenetic tree, but a phylogenetic analysis of all suboscine passerines (Harvey et al., in review) utilized multiple fossil calibrations across passerine birds to date their phylogeny, which included samples of *Epinecrophylla*. From that study we obtained the estimate for the crown age of *Epinecrophylla* (9.28 Ma, 95% CI: 8.60–11.07 Ma) and the divergence times between *Epinecrophylla* and our two outgroup taxa *Neoctantes niger* (13.83 Ma, 95% CI: 12.62–16.22 Ma) and *Myrmorchilus strigilatus* (14.90 Ma, 95% CI: 13.67–17.54 Ma). We used these three date estimates as calibrations to date our phylogenetic tree in treePL (Smith and O'Meara, 2012), which uses penalized likelihood to obtain divergence date estimates for large phylogenies. We ran the treePL analysis using the tree estimated in ExaBayes from the 75% complete dataset, selecting one allele per individual. We set an initial smoothing parameter of 100 and estimated the best optimization parameters with the *prime* function. We used the random subsample and replicate cross-validation function to estimate the optimal smoothing parameter, and then ran the analysis until convergence with this smoothing parameter. We visualized the resulting tree in FigTree 1.4.4 (Rambaut, 2009).

Because absolute rates of mitochondrial sequence evolution (the "mitochondrial clock") are better understood than those of UCE loci, we also estimated a time-calibrated phylogenetic tree in BEAST 2.5.2 (Bouckaert et al., 2019) with our draft mitochondrial genome sequence data and widely used mitochondrial substitution rates. For each of the 13 protein-coding mitochondrial genes we estimated the best model of rate variation in PartitionFinder 2.1.1 (Lanfear et al., 2012), applied these site models to each gene, and linked tree models across partitions. We utilized a mutation rate of 0.01105 substitutions/site/million years (with a standard deviation of 0.0034) for the mitochondrial Cytochrome *b* (cyt b) gene, based on fossil calibrations in birds (Weir and Schluter, 2008) that has been used in suboscine birds (Sousa-Neves et al., 2013). A gamma-distributed uncorrelated log-normal relaxed clock was set on the cyt b mutation rate, and mutation rates for other genes were calculated relative to the cyt b rate. We implemented a birth–death model, with uniform priors of 1 on the birth rate and 0.5 on the death rate, and the same divergence-time prior used in the treePL analysis for the crown age of *Epinecrophylla*. We placed uniform priors of 1 on eighteen transition and transversion rates that failed to converge in initial BEAST runs, and default priors for the remainder. We ran the

analysis for 250 million generations, sampling every 25,000 generations, with a burn-in of 10%, and checked that runs converged in Tracer 1.7.1 (Rambaut et al., 2018) based on ESS values over 200. Two independent runs were combined in LogCombiner 2.5.2, and from the posterior of trees we calculated a maximum clade credibility (MCC) tree in TreeAnnotator 2.5.1, both implemented in Beast 2.5.2 (Bouckaert et al., 2019). We visualized the resulting tree in FigTree 1.4.4 (Rambaut, 2009).

We used SNAPP 1.4.2 (Bryant et al., 2012) implemented in BEAST 2.5.2 (Bouckaert et al., 2019) to calculate a species tree directly from SNP data in a full-coalescent analysis without an outgroup. This site-based method has the advantage of bypassing gene tree estimation and minimizing error due to the low information content of individual UCE loci. SNAPP requires that all samples have data at each locus and that samples be assigned to "species" (i.e. tips), so we employed two sample- and individual-filtering strategies. In both cases we selected from each clade the two individuals (where available) that had the greatest number of UCE loci recovered in order to maximize the number of loci for the SNAPP analyses. In the first analysis we treated as tips each of the clades identified in the ExaBayes 75% phylogeny (Fig. 2) and in the second we treated as tips each widely recognized species in the genus. After selecting individuals for each analysis, we called SNPs following the *seqcap_pop* and SNP filtering pipeline described above, and selected at random one SNP per locus to minimize linkage biases. For each analysis we assigned individuals to population in BEAUti implemented in BEAST 2.5.2 (Bouckaert et al., 2019) and estimated the mutation rates from the data. Based on the tree height of the ExaBayes 75% phylogeny (Fig. S1A) of 0.009 substitutions/site we applied a gamma-distributed prior on the speciation rate ($\lambda = 193$, $\alpha = 2$, $\beta = 250$), and from the average sequence divergence within *Epinecrophylla gutturalis* (0.008%) we applied a gamma-distributed prior on the expected divergence (θ: $\alpha = 2$, $\beta = 250$). We ran all analyses for 2 million generations, storing every 1000 generations, and a burn-in of 10%, and checked that runs converged in Tracer 1.7.1 (Rambaut et al., 2018) based on ESS values over 200. For each analysis, two independent runs were combined in LogCombiner implemented in BEAST 2.5.2 (Bouckaert et al., 2019), and from the posterior of species trees we calculated an MCC tree in TreeAnnotator 2.5.1 implemented in BEAST 2.5.2 (Bouckaert et al., 2019). We used DensiTree 2.0.1 (Bouckaert, 2010) to visualize the posterior tree set of the combined SNAPP runs and FigTree 1.4.4 (Rambaut, 2009) to visualize the MCC trees. Our results from both of these SNAPP analyses showed considerable uncertainty regarding the placement of *pyrrhonota*, *haematonota*, and *fjeldsaai*, so we conducted a third SNAPP analysis in which we restricted our sampling to only the taxa in the *haematonota* group (i.e. those three taxa plus *gutturalis*, *spodionota*, *sororia*, *amazonica*, and *dentei*). With this reduced sampling we called SNPs again and ran a SNAPP analysis using the methods described above, changing only the priors on the speciation rate ($\lambda = 193$, $\alpha = 2$, $\beta = 550$) and the expected divergence ($\alpha = 2$, $\beta = 550$) due to the lower tree height of 0.0036 substitutions/site.

In addition to the analyses outlined above, we conducted a variety of phylogenetic analyses, each with its own assumptions, strengths, and weaknesses relative to treating sources of phylogenetic variation. Details and results for these analyses are available in the Supplementary Materials.

2.7. Population genetics and introgression

In addition to our phylogenetic analyses, we utilized our SNP datasets to investigate patterns of population-level genetic structure and also introgression within and between clades. We used STRUCTURE (Pritchard et al., 2000) and Discriminant Analysis of Principal Components (DAPC) to analyze patterns of population structure within each clade, and implemented each analysis on all six clade-level SNP datasets described in section 2.5. For STRUCTURE, we analyzed the linked SNP datasets and implemented the *linked* model, providing the distance in base pairs between SNPs within each locus, and ran each analysis for 2 million generations, discarding the first 50,000 as burn-in. We ran 10 replicate analyses for each value of K from one to 10, or until the likelihood value of K decreased drastically. We selected the best K value based on the ΔK method of Evanno (Evanno et al., 2005), implemented in STRUCTURE HARVESTER (Earl and vonHoldt, 2012). DAPC uses sequential k-means clustering of principal components to infer the number of genetic clusters in a dataset. We conducted a DAPC analysis in *adegenet* (Jombart and Ahmed, 2011), following the recommendations of Jombart et al. (2010), and selected the best number of clusters based on the lowest Bayesian Information Criterion (BIC) score. In addition, we conducted a Principal Components Analysis (PCA) analysis, with samples coded by DAPC group assignments. Although BIC scores for the *haematonota s.l.* clade indicated that K values greater than 2 had a worse fit to the data than $K = 2$, we calculated DAPC group assignments for K values from 3 to 5 to investigate finer-scale patterns of population structure, due to the greater number of described taxa in this clade.

Pairwise sequence divergence is frequently used to estimate the genetic distinctiveness of bird taxa and to assess taxonomic rank. To this end, we calculated pairwise distance estimates between all taxa in the genus using both the mitochondrial and nuclear DNA data. For the mitochondrial distances we used a concatenated alignment of the 13 mitochondrial protein-coding genes and report genetic distances accounting for multiple substitutions and as the uncorrected *p*-distance. On a neighbor-joining tree reconstructed from the raw *p*-distance matrix in PAUP* 4.0 (Swofford, 1999), we estimated the proportion of invariant sites (0.590355) and the gamma shape parameter (1.82626). These values were then fixed for calculations of a distance matrix under the GTR + γ + I finite-sites substitution model. For the nuclear data we estimated the weighted fixation index (F_{st}) between each pair of taxa using the method of Weir and Cockerham (1984) implemented in vcftools 0.1.16 (Danecek et al., 2011) using the unlinked SNP dataset. For all calculations we also report the average within-taxon distance estimates as a measure of intra-specific genetic structure.

3. Results

3.1. Sequencing results and sample identification

Illumina sequencing of UCEs resulted in an average of 3.8 million reads per individual, and an average read length of 130 bp after trimming. After removing potentially contaminated or misidentified samples, our dataset contained 63 *Epinecrophylla* samples and two outgroups. Including the three potentially contaminated *Epinecrophylla* samples (based on BOLD results) in a phylogenetic tree estimated in RAxML 8.2.12 (Stamatakis, 2014), two grouped with the correct taxon but sat on abnormally long terminal branches, suggesting contamination, and a third grouped with the outgroup samples, suggesting sample misidentification (Fig. S1H). After assembly and locus filtering we obtained an average of 2195 UCE loci per sample (range 1234–2306 loci), with a mean locus length of 652 bp (range 234–1283 bp) and mean read depth of UCE loci of 22.5x (SD: 43.0x). Missing data had a strong effect on the number of UCE loci retained in the alignment, and the alignment that included no missing data contained 330 UCE loci and was not analyzed further. The 95% complete phased alignment contained 1659 UCE loci and an aligned matrix of 1,140,275 bp, and the 75% complete phased alignment contained 2149 UCE loci and an aligned matrix of 1,401,699 bp.

We obtained partial or complete mitochondrial genomes for 59 ingroup samples and two outgroups, including at least one sample per *Epinecrophylla* species (Table S2). Three samples, including one of the outgroups, contained greater than 40% missing data and were removed from the analysis (Table S2). The average mitochondrial genome size was 17,253 bp (range 16,017–17, 930 bp) and had a mean read depth

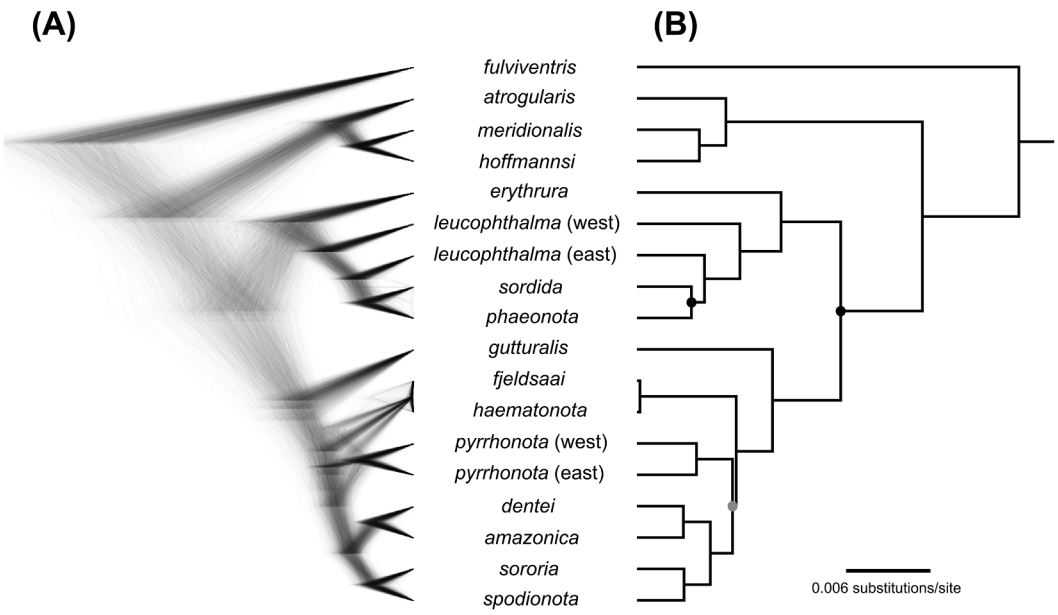

Fig. 3. Species tree estimated in SNAPP from SNP data, with tips representing all named taxa and divergent clades identified from the tree in Fig. 2. A) The DensiTree representation of the posterior distribution of species trees and B) the Maximum Clade Credibility species tree. All nodes received full support unless marked with a circle. Nodes with a posterior probability > 0.95 are marked with a black circle, and the node marked with a gray circle received a posterior probability of 0.49.

of 304.4x (SD: 780.0x). The aligned dataset of 56 individuals using the 13 mitochondrial protein-coding genes was 11,488 bp in length (range 9921–11,396 bp) and contained 4.8% missing data.

3.2. Phylogenetic estimation

From the nuclear UCE data, we recovered a phylogeny with strong support for relationships among taxa (Fig. 2, Fig. 3, Fig. S1). The deepest split in the tree occurred across the Andes, dividing *E. fulviventris* from the remainder of the genus (Fig. 1A, Fig. 2A). Although our sampling included just two samples of *E. fulviventris*, one of which (sample #1) is from a population occasionally separated as the subspecies *costaricensis* (del Hoyo et al., 2019; Todd, 1927), our phylogenies indicated a relatively shallow divergence between the two samples (Fig. S1). The next split separated *E. ornata* from the remaining taxa (Fig. 1A, Fig. 2A). Although we lacked samples for two taxa within this species (*saturata* and nominate *ornata*), the two parapatric gray-backed taxa occurring in Peru (*meridionalis* and *atrogularis*) were recovered as non-sister lineages, with the southern *meridionalis* sister to the rufous-backed *hoffmannsi* of eastern Brazil, and *atrogularis* sister to those two. The next split contained the sister species *E. erythrura* and *E. leucophthalma*, which together are sister to the remaining taxa in the genus (Fig. 1B, Fig. 2A). These two species (*E. erythrura* and *E. leucophthalma*) are reciprocally monophyletic, but within *E. leucophthalma* we recovered the nominate subspecies as paraphyletic. Within this nominate subspecies of *E. leucophthalma*, the western populations (samples #13–16) showed a deep divergence from the remainder of the species. This final group is the *haematonota s.l.* clade, which contains eight largely parapatric taxa (*gutturalis*, *dentei*, *amazonica*, *spodionota*, *sororia*, *pyrrhonota*, *haematonota*, and *fjeldsaai*) that together range across the majority of the Amazon Basin (Fig. 1C, Fig. 2A). The Guiana Shield taxon *E. gutturalis* is sister to the rest of the taxa in this clade, but contains minimal genetic structure in the phylogeny (Fig. 2). The remaining taxa can be divided into three groups with similar divergence times between them (Fig. 2A). The first group contains the southeastern Amazonian *E. amazonica* (including the subspecies *dentei*) and the Andean foothill *E. spodionota* (including the subspecies *sororia*), the second is the northwestern Amazonian taxon *pyrrhonota*, and the third is the western Amazonian *E. haematonota* (including the subspecies *fjeldsaai*). The taxon *fjeldsaai* was embedded within *haematonota* in all analyses, thus rendering *haematonota* paraphyletic. Our UCE phylogeny placed *pyrrhonota* sister to *haematonota*, with *amazonica* and *spodionota* sister to those two. Analyses of nuclear data with a variety of phylogenetic methods (see Supplementary Material) largely supported the above results. However, analysis of mitochondrial data (Fig. 2B, Fig. 4) and some analyses of nuclear data (Fig. 4) indicated support for two alternate topologies with regard to the placement of these three clades, both of which indicated a non-sister relationship between *haematonota* and *pyrrhonota*, though with varying degrees of node support (Figs. S1, S2). Aside from these topological discordances, the mitochondrial and nuclear phylogenies were largely concordant, albeit with lower node support in some parts of the mitochondrial phylogeny. The mitochondrial phylogeny (Fig. 2B) differed from the nuclear phylogeny in suggesting paraphyly in both *E. leucophthalma sordida* and in the eastern clade of nominate *leucophthalma*, monophyly of both subspecies of *E. spodionota*, and support for two recently diverged clades within *E. haematonota*. The two mitochondrial clades of *E. haematonota* correspond to 1) samples south and east of the Rios Amazonas and Ucayali and 2) samples from west of the Rio Ucayali and all samples of *fjeldsaai*. Both nuclear and mitochondrial analyses showed two clades within *pyrrhonota*, which split one sample from west of the Rio Japurá from those to the east of the river.

Date estimates of most nodes from UCE and mitochondrial data (Fig. 2) were largely concordant, suggesting that the four major clades of *Epinecrophylla* (*fulviventris*, *ornata*, *leucophthalma/erythrura*, and *haematonota s.l.*) diverged in the late Miocene between 7 and 10 Ma, while most species-level divergences occurred in the Pliocene between 2 and 5 Ma. However, intra-specific divergence estimates (i.e. more recent splits) in the mitochondrial phylogeny were lower than those in the UCE phylogeny, and may be more reasonable date estimates given the low information content of UCE loci and the population-level sampling in this project. Both phylogenies suggested that the oldest splits within *E. ornata* and *E. leucophthalma* are as old or older than some of the species-level splits within the *haematonota s.l.* clade.

Both the species-level and clade-level MCC phylogenies estimated in SNAPP (Fig. 3, Fig. S3) produced topologies broadly concordant with those recovered in our dated phylogenetic analysis of UCE data. However, in both SNAPP analyses the DensiTree representation of the

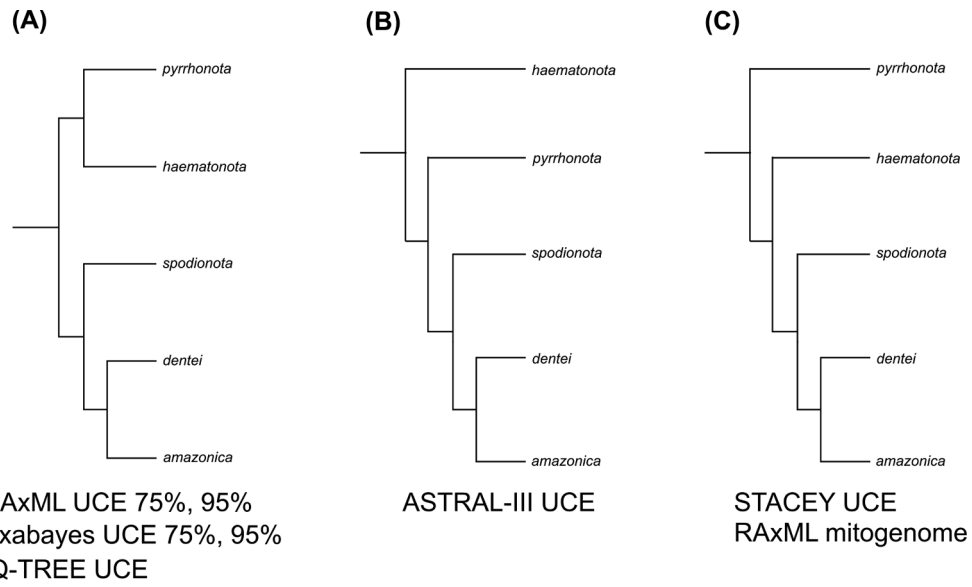

Fig. 4. Alternate topologies recovered across phylogenetic methods for relationships within the *Epinecrophylla haematonota s.l.* clade. Results are shown using a single individual per taxon for visualization purposes. In all cases *E. haematonota fjeldsaai* was recovered as embedded within *E. h. haematonota* and is not shown. The methods recovering each topology are shown below the topology, and the full phylogenies using each method are in Fig. S1. SNAPP analyses recovered all three topologies shown here (see text for details).

posterior of species trees showed three distinct topologies for the relationship between *pyrrhonota, E. haematonota,* and *E. amazonica/E. spodionota*, and in both cases each of these three topologies comprised approximately equal proportions of the posterior of species trees (range 19–53%). The three topologies recovered by SNAPP are those shown in Fig. 4, but the topology with the greatest support differed between analysis. The presence of these alternate topologies was reflected in low statistical support for these nodes in the MCC phylogenies. The phylogeny estimated in SNAPP using samples from only taxa in the *haematonota s.l.* clade recovered an MCC tree with very high statistical support and the DensiTree representation of the posterior of species trees showed a single topology (Fig. S4, the topology shown in Fig. 4C) that indicated a non-sister relationship between *pyrrhonota* and *haematonota/fjeldsaai*.

3.3. Population genetics

DAPC analyses with k-means cross-validation estimated a best fit model of K = 2 for each of three clades: *E. leucophthalma*, *E. ornata*, and *haematonota s.l.*, and a model of K = 1 for *E. gutturalis* (Fig. 5). For *E. leucophthalma* this divided the species into the "*leucophthalma* west" clade (samples #13–16) and the remainder of the eastern taxa, including the "*leucophthalma* east" clade. For *E. ornata*, DAPC separated the central Peruvian *atrogularis* from the two eastern taxa. Lastly, for the *haematonota s.l.* clade, the best fit model of K = 2 separated *pyrrhonota* from the remainder of the group. The worse-fit models of K > 2 (based on BIC scores) for the *haematonota s.l.* clade (sans *E. gutturalis*) first separated the *E. spodionota/E. amazonica* clade at K = 3, then *E. spodionota* from *E. amazonica* at K = 4, and the western-most sample (#54) of *E. h. pyrrhonota* at K = 5. PCA plots with points labeled by taxon and sample number are shown in Fig. S5.

STRUCTURE results largely recapitulated those from DAPC (Fig. 5) but provided a more in-depth view of individuals with potential genetic backgrounds from multiple populations (i.e. potential introgression). Results from the Evanno method based on the ΔK value were unambiguous in all cases. However, in all cases the STRUCTURE plot for the "best" value of K from the Evanno method added a population that was approximately evenly assigned across all individuals. Therefore, we consider the STRUCTURE plot for the "best" K minus 1 to be a more biologically realistic representation of the data and report all STRUCTURE plots > 1 that have high likelihood values, following the recommendation of Meirmans (2015). Because the Evanno method is unable to calculate a ΔK value at K = 1 and because all individuals of *E. gutturalis* were approximately equally assigned to both populations at K = 2, we consider a K = 1 to be the best-fit model for that species. For *E. leucophthalma*, K = 2 separated the "*leucophthalma* west" clade from the remainder of the eastern taxa, but with all individuals containing a small percentage of genetic membership from the other clade. Within *E. ornata*, results were similar to those of DAPC, with *atrogularis* the most distinct at K = 2, but with all individuals having a proportion of their ancestry assigned to both populations. The pattern in the STRUCTURE plots for the *haematonota s.l.* clade (sans *E. gutturalis*) was more complex. At K = 2, STRUCTURE assignments largely separated *E. h. pyrrhonota* from *E. spodionota/E. amazonica*, with all individuals of the *E. h. haematonota/E. h. fjeldsaai* group having about equal ancestry between the two groups. This pattern was also reflected also in the intermediate position of the *E. h. haematonota/E. h. fjeldsaai* group along the first principal component of the PCA results. At K = 3, STRUCTURE separated three groups that corresponded to taxonomy, with most individuals showing only a small proportion of shared population assignments: 1) *E. h. pyrrhonota*, 2) *E. spodionota/E. amazonica*, and 3) *E. h. haematonota/E. h. fjeldsaai*. The "best" value of K = 4 provided only a slight suggestion of differentiation between *E. spodionota* and *E. amazonica*, with *E. a. dentei* genetically indistinguishable from *E. a. amazonica,* and *E. s. sororia* genetically indistinguishable from *E. s. spodionota*.

The genetic distance estimates largely corroborate the phylogenetic patterns of genetic distinctiveness and population structure from our dated phylogeny. The full results for the mitochondrial and nuclear distances are shown in Tables S3 and S4, respectively, but select results are worth reporting here. Consistent with the paraphyly in our phylogenetic results, we found that *fjeldsaai* was largely undifferentiated from *haematonota* (corrected mtDNA 0.8%, F_{st} 0.02). In contrast, we found *pyrrhonota* to be nearly as distinct from *E. haematonota* (corrected mtDNA 5.7%, F_{st} 0.24), with which it is currently considered conspecific, as from *E. amazonica* (corrected mtDNA 6.0%, F_{st} 0.34) or *E. spodionota* (corrected mtDNA 6.1%, F_{st} 0.34). Likewise, the average intra-specific distances for *E. ornata* (corrected mtDNA 3.1%, F_{st} 0.30) and *E. leucophthalma* (corrected mtDNA 2.8%, F_{st} 0.30) are strongly suggestive of species-level divergences within both of these groups (Fig. S8). The distance between *E. a. amazonica* and *E. a. dentei* (corrected mtDNA 2.8%, F_{st} 0.19) is inconclusive with regards to species status.

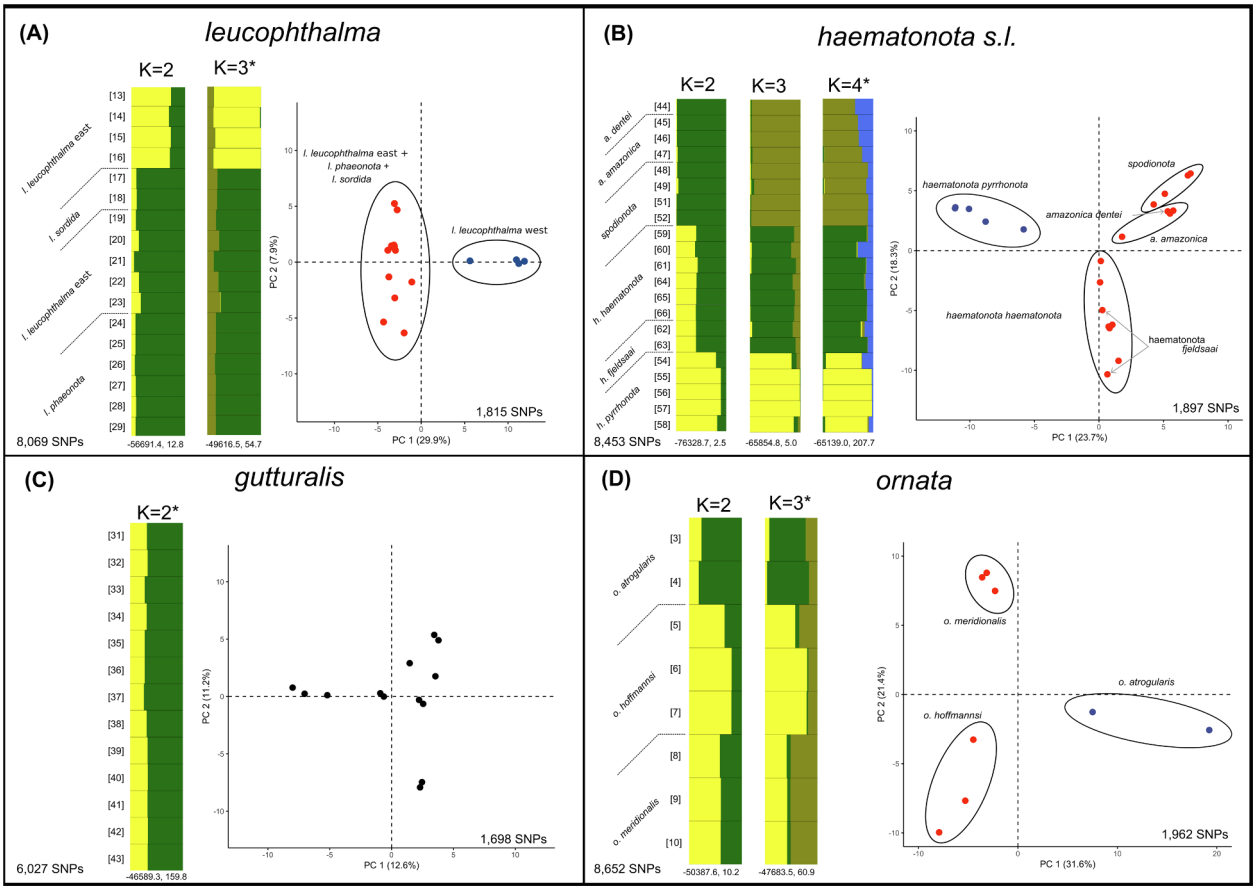

Fig. 5. Intra-specific population genetic analyses. A) *Epinecrophylla leucophthalma,* B) the *E. haematonota s.l.* clade, containing *dentei*, *amazonica*, *spodionota*, *sororia*, *pyrrhonota*, *haematonota*, and *fjeldsaai*, C) *E. gutturalis*, and D) *E. ornata*. For each section is shown a Principal Components Analysis (PCA) with samples colored by the Discriminant Analysis of Principal Components Analysis (DAPC) group assignments on the right, and STRUCTURE plots for all likely values of K (i.e. those with low standard deviation across replicate runs) on the left. Not shown are results for K = 1. The plot for the "best" value of K for each clade using the Evanno method is marked with an asterisk. Mean log likelihood and delta K values are shown below each STRUCTURE plot. Sample size in PCA plots refer to the number of unlinked SNPs recovered in that clade and used in the PCA analysis. Blue and red circles denote group assignments from DAPC while black circles and text denote taxa. Sample numbers correspond to those in Fig. 1 and Table 1. PCAs with sample numbers included are shown in Fig. S6. (For interpretation of the references to color in this figure legend, the reader is referred to the web version of this article.)

4. Discussion

4.1. Phylogeny and population genetics

Our analyses of nuclear and mitochondrial data largely resolved the evolutionary relationships among *Epinecrophylla* taxa and recovered three broadly sympatric species complexes in the Amazon Basin. We consider the topology of the phylogeny illustrated in Fig. 2A to be the best representation of relationships in the group based on the consistently high support values across multiple methods that recovered this topology (Fig. 3, Fig. 4, Fig. S1A-D, Fig. S1G). There was, however, some disagreement among methods and data types regarding the placement of taxa in the *haematonota* group (Fig. 3, Fig. 4), with some methods suggesting a non-sister relationship between *pyrrhonota* and *haematonota*. Most of the nuclear topologies that disagreed with the sister relationship of *pyrrhonota* and *haematonota* received low support for that node, often in conjunction with a very short subtending branch (Fig. S1E-F). These short branches suggest that the divergence between the three primary lineages in the *haematonota s.l.* clade was likely very rapid, which combined with the effects of incomplete lineage sorting and perhaps hybridization, may explain the conflicting signal across methods and the support for alternate topologies in the SNAPP posterior species tree distributions (Fig. 3A, Fig. S3A).

Because a strictly bifurcating tree is likely not an appropriate model for intraspecific relationships in cases of high levels of gene flow (Eckert and Carstens, 2008), our population genetics results may be a better representation of the evolutionary relationships among individuals at this fine scale. The evolutionary patterns recovered with these population genetics analyses indicate little differentiation between most subspecies and even between some taxa currently recognized as species (e.g. *E. spodionota* and *E. amazonica*). The three Amazonian species complexes that we recovered in our phylogeny are sympatric across much of the western Amazon Basin, but are represented by one species each in the eastern parts of the Amazon Basin. These species complexes are 1) *E. ornata*, 2) *E. leucophthalma* and *E. erythrura*, and 3) the *haematonota s.l.* group. Each complex contains taxa that are either allopatric or largely parapatric, with distributions typically bounded by large rivers (Fig. 1). We discuss the phylogenetic results and taxonomic implications of each species or species group separately. Taxa marked with an asterisk are considered synonyms by some authors.

4.2. Epinecrophylla fulviventris

Taxa included: *fulviventris* (Lawrence, 1862), *salmoni** (Chubb, 1918), and *costaricensis** (Todd, 1927).

Epinecrophylla fulviventris was recovered as sister to the remainder of the genus in all analyses and with relatively shallow divergence between our two samples in most phylogenies. We lack the geographic sampling or morphological data to make any taxonomic recommendations for this species, and thus suggest maintaining the current

treatment of a monotypic *E. fulviventris* following recent authors (Clements et al., 2019; Zimmer and Isler, 2003).

4.3. Epinecrophylla ornata

Taxa included: *ornata* (Sclater, 1853), *atrogularis* (Taczanowski, 1874), *hoffmannsi* (Hellmayr, 1906), *saturata* (Chapman, 1923), and *meridionalis* (Zimmer, 1932).

The only predominantly gray-bodied species in the genus, our results for this morphologically distinctive group are hampered by the lack of samples of the nominate taxon and the geographically adjacent taxon *saturata*. The species was described from a "Bogota" skin and is thus of uncertain provenance, although typically assumed to be from the lowlands of southern Amazonian Colombia (Peters, 1951). However, without samples from Ecuador or southern Colombia, we are unable to fully resolve the relationships within this species or recommend taxonomic changes. Despite the lack of these samples, we discovered deep splits and high population structure among all three subspecies in our phylogenetic analyses, suggesting that multiple species-level taxa occur in the group. The most genetically distinct of the three taxa in phylogenetic and population genetic analyses was *atrogularis* of central Peru, which all analyses placed as sister to *meridionalis/hoffmannsi*, thus contradicting the opinion of some authors (e.g. del Hoyo et al., 2019) that *hoffmannsi* represents a species distinct from the other four taxa in *E. o. ornata*. This relationship is surprising given the phenotypic similarity of *atrogularis* and *meridionalis*, which both lack the rufous back of the other three taxa in the *ornata* group and differ from each other primarily in the slightly brighter brown upperparts of female *meridionalis*, while the males are largely indistinguishable (Zimmer, 1932b). *E. o. atrogularis* and *E. o. meridionalis* potentially come into contact in the Ucayali Region of southern Peru, and further research on this contact zone is of interest given the deep genetic split between the two taxa presented here. Reports of specimens of male *meridionalis* with some rufous on the back from southern Peru in Cusco and Madre de Dios Regions have been suggested to be either variation within *meridionalis* or evidence of introgression with one of the rufous-backed forms (Ridgely and Tudor, 1994). We suspect that the latter is a more likely explanation, based on the population genetic STRUCTURE results (Fig. 5D) that show individuals with shared population assignments between all three subspecies that we sampled, despite the deep genetic splits among them.

4.4. Epinecrophylla leucophthalma and E. erythrura

Taxa included in *E. leucophthalma*: *leucophthalma* (von Pelzeln, 1868), *phaeonota* (Todd, 1927), *sordida* (Todd, 1927), and *dissita* (Bond, 1950).

Taxa included in *E. erythrura*: *erythrura* (Sclater, 1890) and *septentrionalis* (Zimmer, 1932).

Ours is the first study to suggest a sister relationship between these two species. The split between the two species is quite deep, and the two species have largely parapatric distributions, but are locally sympatric in Peru (Fig. 1B; Schulenberg et al., 2007; Álvarez Alonso, 2002) without showing any morphological signs of introgression, thus confirming their status as species. Notably, we found that the nominate subspecies of *E. leucophthalma* is paraphyletic as currently recognized, with western populations of *E. l. leucophthalma* sister to a group containing the subspecies *sordida* and *phaeonota* and the eastern populations of the nominate subspecies. This deep genetic divergence within *E. leucophthalma* is comparable to some divergences among taxa considered to be species within the *haematonota s.l.* clade, in particular between *E. spodionota* and *E. amazonica*, but to our knowledge no morphological characters have been proposed to diagnose this western population of *E. leucophthalma*. Excluding that western population, the remainder of the *E. leucophthalma* samples in our analysis showed extremely low divergence among them, although most of our nuclear phylogenies grouped samples into three shallowly diverged groups corresponding to *sordida*, *phaeonota*, and the eastern clade of *leucophthalma*. Because the geographically intermediate taxon *phaeonota* is morphologically distinctive (rufous back in *phaeonota* vs brown in all other *leucophthalma* taxa), we support the continued treatment of the three *leucophthalma* taxa as separate subspecies despite the very low genetic divergence between them. This treatment is further supported by the presence of specimens intermediate between *leucophthalma* and *phaeonota* on the Río Roosevelt (Zimmer, 1932a). The type locality of *E. leucophthalma* is on the right bank of the Río Madeira at Salto do Jirau, Rondônia, Brazil (von Pelzeln and Natterer, 1871), in the same interfluve and just 150 km to the north of our sample #20 (Fig. 1B), thus suggesting that the name *leucophthalma* applies to the eastern clade of *E. l. leucophthalma* and that the Río Madeira may correspond to the deep genetic break within the species. The southern Andean foothill taxon *dissita* comes into contact with our western clade of *E. l. leucophthalma* in southern Peru (Fig. 1B), so the name *dissita* could potentially be expanded to include the rest of Peru and Pando, Bolivia (i.e. our "*leucophthalma* west" clade). Alternatively, a new name might be necessary for this western population of *E. l. leucophthalma*. However, genetic samples of *dissita* are needed to confirm which of these alternative treatments is appropriate. Estimates of the finite-sites mitochondrial distance and weighted nuclear F_{st} between the western clade of *E. l. leucophthalma* and all eastern populations are 6.3% and 0.29, respectively (Table S3, S4).

4.5. Epinecrophylla haematonota group

Taxa included in *E. haematonota*: *haematonota* (Sclater, 1857) and *fjeldsaai* (Krabbe, Isler, Isler, Whitney, Alvarez, & Greenfield, 1999).

Taxa included in *E. spodionota*: *spodionota* (Sclater & Salvin, 1880) and *sororia* (von Berlepsch & Stolzmann, 1894).

Taxa included in *E. amazonica*: *amazonica* (von Ihering, 1905) and *dentei* Whitney, Isler, Bravo, Aristizábal, Schunck, Silveira, & de Q. Piacentini, 2013.

Monotypic species: *E. pyrrhonota* (Sclater & Salvin, 1873) and *E. gutturalis* (Sclater & Salvin, 1881).

This clade contains eight taxa that have undergone many taxonomic rearrangements throughout their history (Cory and Hellmayr, 1924; del Hoyo et al., 2019; Dickinson and Christidis, 2014; Isler and Whitney, 2018; Peters, 1951; Remsen et al., 2019; Whitney et al., 2013; Zimmer, 1932a; Zimmer and Isler, 2003). Our phylogenetic analyses indicate that *E. gutturalis* is part of this species complex and is sister to the rest of the clade. All of our phylogenetic and STRUCTURE analyses showed no population structure within *E. gutturalis* across its range. DAPC results showed low levels of structure, but still indicated a K = 1 based on BIC scores. The five samples that showed slight divergence from the main cluster in the PCA results (Fig. 5C; sample numbers 32, 34, 35, 36, and 40) did not cluster based on geography. The close relationship and relatively shallow divergence between *E. spodionota* (including *sororia*) of the Andean foothills and *E. amazonica* (including *dentei*) of the southern Amazonian lowlands presents an interesting biogeographic pattern that is uncommon among birds, and received high statistical support across our phylogenetic analyses. Aside from the placement of *E. gutturalis*, we found considerable disagreement across phylogenetic methods regarding the relationships between the three other main clades in this group, namely *E. pyrrhonota* of northwestern lowland Amazonia, *E. haematonota* (with *fjeldsaai* phylogenetically embedded within *haematonota*) of western lowland Amazonia, and *E. amazonica/E. spodionota*, despite relatively old divergence times between the three clades. Most phylogenetic analyses of UCE data indicated a sister relationship between *pyrrhonota* and *haematonota* (e.g. Fig. 2, Fig. 4, Fig. S4A), but multiple methods indicated a non-sister relationship between the two lineages, with either *haematonota* or *pyrrhonota* sister to the *E. amazonica/E. spodionota* clade depending on the analysis (Fig. 4), in some cases with high statistical support. Regardless of the topology

recovered, most phylogenetic results indicated very short branches separating the divergence of each of these three clades. Such short internodes have proven difficult to resolve even with many thousands more loci than we have analyzed here (e.g. Cheng et al., 2020), but even by doubling the number of loci analyzed – albeit with fewer samples – (see Supplementary methods) we recovered the same topology as is shown in Fig. 2A (Fig. S1H). Additional studies with more loci, and in particular more data types, are desirable to fully resolve these relationships and to determine the extent to which incomplete lineage sorting, hybridization, or other factors are responsible for the topological uncertainty in our phylogenetic results. A relatively deep phylogenetic break between our eastern and western samples of *E. pyrrhonota*, perhaps across the Rio Japurá, is also worthy of additional investigation. The only known sympatry between any taxa in this group occurs on the east slope of the Andes in southern Colombia where Salaman et al. (2002) reported *pyrrhonota* and *spodionota* being captured in the same mist-nets, thus necessitating at a minimum the separation of *E. pyrrhonota* and *E. amazonica/E. spodionota* as biological species. Given the similarly old divergence times between 1) *E. pyrrhonota*, 2) *E. amazonica/E. spodionota*, and 3) *E. haematonota* (all ~ 2.5–3 Ma) we believe that these three lineages each represent separate biological species. Additionally, *E. amazonica* and *E. spodionota* are widely considered to be separate species based on differing morphology and habitat, and our genetic results are consistent with that treatment.

Isler et al. (1998) developed a yardstick system based on vocalizations to evaluate species limits in Thamnophilidae. Isler and Whitney (2018) applied this system to *haematonota*, *pyrrhonota*, and *fjeldsaai*, finding that the three taxa did not differ in vocalizations and were therefore best regarded as three subspecies of *E. haematonota*. Our results suggest that the divergence between *pyrrhonota* and *E. amazonica/E. spodionota* (mtDNA 6.1%, weighted F_{st} 0.34) is comparable to that between *pyrrhonota* and *haematonota/fjeldsaai* (mtDNA 5.7%%, weighted F_{st} 0.25), and some analyses indicate a non-sister relationship between *pyrrhonota* and *haematonota/fjeldsaai* (Fig. 2B, Fig. 3, Fig. 4, Fig. S3). This, combined with the results from our DAPC and STRUCTURE analyses which indicate that *pyrrhonota* is the most divergent taxon in this group, and in particular much more so than *E. amazonica* is from *E. spodionota*, that *E. pyrrhonota* is best regarded as a distinct species. A more thorough evaluation of the utility of this yardstick system between all *Epinecrophylla* taxa is desirable, but the results presented here indicate that the Isler et al. (1998) vocalization-based yardstick system may not be a reliable indicator of species status in this genus.

Our results support the continued treatment of *fjeldsaai* as a subspecies of *E. haematonota* due to its morphological distinctiveness despite its low genetic differentiation, but were more ambiguous with regard to the taxonomic status of *dentei*. None of our population genetics analyses were able to differentiate *fjeldsaai* from *haematonota*, and all phylogenetic analyses indicated that *fjeldsaai* was embedded within *haematonota*. This treatment is further supported by evidence of hybridization between the two taxa in northwestern Peru (LSUMNS specimens). In fact, one of our samples of *fjeldsaai* (sample #62) has some rufous coloration on the lower back suggestive of hybridization with *haematonota*. Remarkably, Zimmer (1932b) presciently noted that the presence or absence of rufous on the back may not be a reliable species-level character in this genus, and our genetic data support that conclusion. In contrast, *dentei* was placed as sister to *E. amazonica* in all phylogenetic analyses, but with relatively shallow divergence (mtDNA 2.8%, weighted F_{st} 0.19) that is less than that shown by population-level or subspecies-level divergences of some other species in the genus. However, we note that many bird species show much lower genetic divergence than that of *dentei*, and that this comparison may rather provide evidence for multiple species-level taxa within some of these other species of *Epinecrophylla*. Our population genetics analyses including all samples in the *haematonota s.l.* clade were unable to distinguish *amazonica* and *dentei* (Fig. 5), and in fact were largely unable to differentiate *E. amazonica* and *E. spodionota*. However, a DAPC analysis using just the three samples of *amazonica* and the one of *dentei* did suggest a K = 2 was the best model based on BIC scores and separated the *dentei* sample from the rest of *amazonica* (Fig. S6).

In summary, we recommend the following 5-species treatment for the taxa in the *haematonota* group: *E. gutturalis*, *E. haematonota* (with *fjeldsaai* as a subspecies), *E. pyrrhonota*, *E. amazonica* (with *dentei* as a subspecies, or potentially as its own species), and *E. spodionota* (with *sororia* as a subspecies). Until genetic samples of *E. leucophthalma dissita*, *E. ornata ornata*, and *E. o. saturata* are available for study, we refrain from making taxonomic recommendations in those groups, but we suspect that both *E. leucophthalma* and *E. ornata* contain multiple species-level taxa. Therefore, we recommend the following species-level linear taxonomy for *Epinecrophylla*: *fulviventris*, *ornata*, *erythrura*, *leucophthalma*, *gutturalis*, *haematonota*, *pyrrhonota*, *amazonica*, *spodionota*.

4.6. Biogeographic patterns

Having three broadly sympatric species or species complexes distributed across the Amazon Basin provides replicated evolutionary histories across a shared landscape. Of interest is the response of each of these species or species complexes to well-known biogeographic barriers in the Amazon Basin, such as large rivers (Capparella, 1991; Wallace, 1854). The major river systems of the Amazon Basin – such as the Solimões, Negro, and Madeira – all appear to have an effect on the genetic structure and range limits of *Epinecrophylla* taxa, delimiting many species and subspecies that show significant genetic breaks at those locations in our analyses. Smaller river systems, however, appear to have idiosyncratic effects on genetic structure, with some delimiting genetic groups in one species, but having little to no effect in others. For example, the Río Purús is a major barrier for *E. ornata*, but has little effect on the genetic structure of other groups, while the Río Tapajós is a barrier for subspecies of *E. leucophthalma* but not *E. ornata*.

The distribution and genetic boundaries of phenotypically distinctive taxa such as *fjeldsaai* and *phaeonota* do not appear to always follow biogeographic barriers that affect other bird species. The brown-backed *fjeldsaai*, which we find to be phylogenetically embedded within the rufous-backed *haematonota*, hybridizes with *haematonota* within the Napo interfluve without any clear biogeographic barrier separating the two taxa. Likewise, the rufous-backed *phaeonota* is part of the otherwise brown-backed *E. leucophthalma*, and appears to replace the eastern populations of nominate *leucophthalma* somewhere between the Juruena and Roosevelt rivers, and specimens with intermediate plumage have been noted (Zimmer, 1932a). It is worth mentioning that while *fjeldsaai* and *phaeonota* are phenotypically distinctive within their respective clades, our analyses indicate that they are not genetically sufficiently distinctive to be considered species, perhaps because they are not separated from adjacent taxa by prominent biogeographic barriers such as rivers that would allow for the buildup of fixed genetic differences concordant with their morphological differences.

That two species complexes – *E. ornata* and *E. leucophthalma/E. erythrura* – are absent from the Guiana Shield and the northern half of the Inambari interfluve (Fig. 1A, 1B) is perplexing. Likewise, the *haematonota* group is absent from the Brazilian Shield, while the other two species complexes are present there. These patterns may be due to the vagaries of extinction, interspecific competition, or habitat suitability, or some combination of those factors, all of which require further study. It is possible that suboptimal habitat, either currently or historically, may increase competition between these closely related and ecologically similar species, leading to local extinctions. Quaternary climate fluctuations that resulted in drier conditions in the southeastern Amazon Basin are thought to have negatively impacted populations of humid forest species in this region (Cheng et al., 2013; Baker et al., 2020), and this region is currently drier on average than western and northern parts of the Amazon Basin (Fick and Hijmans, 2017). This

seems unlikely to be the primary driver of distribution patterns in *Epinecrophylla*, as it would explain the absence of any representatives of the *haematonota* group in the southeastern Amazon Basin, but not the presence *E. ornata* and *E. leucophthalma* in the same region. There is, however, evidence that co-occurrence, competition, and habitat segregation may play a role in the ability of *Epinecrophylla* species to coexist over broad spatial scales. Evidence from different localities suggests that spatial variation in habitat preferences is dependent on how many congenerics are present at a locality. In general, *E. ornata* shows a greater affiliation for bamboo habitats, *E. leucophthalma* for second growth or bottomland forest, and the *haematonota* group for upland forest (del Hoyo et al., 2019), but multiple species may be present at a single locality or even a single mixed-species flock. For example, Rosenberg (1997) frequently found *E. leucophthalma* and *E. ornata* in the same mixed flocks at Tambopata, Peru, but *E. ornata* foraged more frequently in bamboo micro-habitats. These two species are reported to segregate by habitat to a greater degree in Mato Grosso, Brazil (del Hoyo et al., 2019). In contrast, J. Tobias (personal communication) found *E. leucophthalma* and *E. amazonica* regularly at the same site in Madre de Dios, Peru, but the two species rarely occurred in the same mixed species flock. Likewise, in Napo, Ecuador, Whitney (1994) found *E. ornata* and *E. erythrura* in the same mixed species flock on just one occasion, although three species of *Epinecrophylla* occurred at the site. However, in cases where one species is absent the others may occupy the habitats typically occupied by the absent species, and Rosenberg (1997) noted that at a site in Pando, Bolivia where *E. ornata* was absent, that *E. leucophthalma* and *E. amazonica* segregated by habitat, with the former utilizing bamboo (a habitat more typical of *E. ornata*) and disturbed habitats and the latter in upland forest. It is unclear to what degree co-occurrence, competition, and habitat preferences are a response to the vagaries of distributional differences among species or whether the reverse is true and these factors drive species distributions. Answers to these questions require further study.

4.7. Areas of potential future research

The results of our phylogenetic and population genetic analyses suggest that multiple geographic regions could produce valuable insights with both greater sampling effort and natural history observations (e.g. playback experiments, surveys of contact zones, analysis of vocal and morphological traits). The first is in southern Peru in the foothills of southeastern Madre de Dios region, where three taxa potentially come into close geographic proximity, namely *E. spodionota, E. amazonica* (which we recover as sister species), and *E. haematonota*. A second region of interest is slightly to the north in southern Ucayali region, where two subspecies of *E. ornata – atrogularis* and *meridionalis* – replace each other, perhaps across the Río Purús, though the two are not recovered as sister taxa in our phylogenies and could come into contact across the headwaters of that river. Genetic samples of the two northern taxa in *E. ornata*, including the nominate subspecies, are critical to resolving relationships within that species. A third region is the headwaters of the Río Napo in northern Ecuador, where two taxa currently regarded as subspecies of *E. haematonota*, *pyrrhonota* and *fjeldsaai* (but see our results regarding the genetic distinctiveness of *pyrrhonota*), could potentially come into contact. Analysis of a contact zone in this region would be critical to resolving species limits in the *haematonota* group.

Despite being the most well-sampled phylogenetic study of *Epinecrophylla* to date, our study lacked genetic samples from some key areas that could affect the results presented here. The lack of samples for two subspecies of *E. ornata*, including the nominate, hinders our ability to make any taxonomic recommendations for that species. We also lack samples of *E. leucophthalma dissita* of the Yungas. This taxon comes into contact with the western clade of nominate *leucophthalma*, and it is possible that the name *dissita* could apply to the entirety of this western clade, a population that based on our results may represent a species distinct from the eastern taxa in *E. leucophthalma*. Two other sampling gaps are worth mentioning; the first is the population of *E. h. haematonota* from the north bank of the Amazon west of the Napo, which is the population that presumably intergrades with *E. h. fjeldsaai*, and the second is a lack of samples for any taxon from the vast region of the Brazilian Amazon west of the Río Madeira and south of the Río Amazonas, which could contain genetically distinct populations and contains the type locality of *E. amazonica* (Peters, 1951).

5. Conclusions

As has been shown in other Neotropical avian systems (Brumfield, 2005; Musher and Cracraft, 2018), our study highlights the importance of sampling populations below the species level, especially in tropical regions, where the taxonomy of many groups is unresolved and there may be considerable undiscovered morphological and genetic diversity. Our understanding of phylogenetic relationships has grown dramatically in recent decades as technological advances have allowed us to obtain and analyze sequence data for ever more genetic markers and individuals, including at the population level in non-model organisms (Harris et al., 2018; Tan et al., 2019; Zarza et al., 2016; Zucker et al., 2016). Applying these new methods to *Epinecrophylla*, we have uncovered novel phylogenetic relationships at the species, subspecies, and population levels, suggesting that the species diversity of this genus has thus far been underestimated.

CRediT authorship contribution statement

Oscar Johnson: Conceptualization, Methodology, Software, Formal analysis, Investigation, Resources, Data curation, Writing - original draft, Writing - review & editing, Visualization, Funding acquisition. **Jeffrey T. Howard:** Conceptualization, Funding acquisition, Investigation, Writing - review & editing. **Robb T. Brumfield:** Conceptualization, Funding acquisition, Resources, Formal analysis, Supervision, Writing - review & editing, Project administration.

Acknowledgements

OJ was supported by the National Science Foundation Graduate Research Fellowship under grant no. DGE-1247192. JTH was supported by the National Science Foundation Research Experiences for Undergraduates under grant no. DEB-1146265. This research was supported in part by NSF grant DEB-1146265 to RTB. The samples from Harvey et al. (in review) were sequenced with FAPESP grant 2012-23852-0 to Gustavo A. Bravo and Brazilian Research Council (CNPq) grant 457974-2014-1 to Gustavo A. Bravo and Luis Fabio Silveira. We thank the curators and staff at the following institutions for providing tissue samples: Gary Graves and Christopher Milensky at the Smithsonian National Museum of Natural History, Richard Prum and Kristof Zyskowski at the Yale Peabody Museum, Christopher Witt at the Museum of Southwestern Biology, Joel Cracraft and Paul Sweet at the American Museum of Natural History, John Bates and Ben Marks at the Field Museum of Natural History, and Rob Moyle and Mark Robbins at the University of Kansas Biodiversity Institute & Natural History Museum. We also thank the numerous field workers who collected the samples used in this study. Donna Dittmann assisted with tissue sample processing at the Louisiana State University Museum of Natural Science. Van Remsen, Daniel F. Lane, Nelson Buainain Neto, and members of the Brumfield Lab provided invaluable feedback on versions of this manuscript. Marco A. Rego aided with the creation of Fig. 1. Louisiana State University High Performance Computing provided computational resources.

Data availability

Raw read data are archived in the Sequence Read Archive under

BioProject number PRJNA622761. All phylogenetic trees, both nuclear and mitochondrial alignments, and BEAST input files are available in Dryad at https://doi.org/10.5061/dryad.r2280gb9n.

Appendix A. Supplementary data

Supplementary data to this article can be found online at https://doi.org/10.1016/j.ympev.2020.106962.

References

Aberer, A.J., Kobert, K., Stamatakis, A., 2014. ExaBayes: massively parallel Bayesian tree inference for the whole-genome era. Mol. Biol. Evol. 31, 2553–2556. https://doi.org/10.1093/molbev/msu236.

Álvarez Alonso, J., 2002. Characteristic avifauna of white-sand forests in northern Peruvian Amazonia. Louisiana, Louisiana State University, Baton Rouge.

Andermann, T., Fernandes, A.M., Olsson, U., Topel, M., Pfeil, B., Oxelman, B., Aleixo, A., Faircloth, B.C., Antonelli, A., 2019. Allele phasing greatly improves the phylogenetic utility of ultraconserved elements. Syst. Biol. 68, 32–46. https://doi.org/10.1093/sysbio/syy039.

Baker, P.A., Fritz, S. C., Battisti, D.S., Dick, C.W., Vargas, O. M., Asner, G.P., Martin, R.E., Wheatley, A., Prates, I., 2020. Beyond refugia: new insights on Quaternary climate variation and the evolution of biotic diversity in tropical South America. In: Rull, V., Carnaval, A.C. (Eds.), Neotropical Diversification: Patterns and Processes. Fascinating Life Sciences, pp. 313–319. http://doi.org/10.1007/978-3-030-31167-4_3.

Bernt, M., Donath, A., Jühling, F., Externbrink, F., Florentz, C., Fritzsch, G., Pütz, J., Middendorf, M., Stadler, P.F., 2013. MITOS: Improved de novo metazoan mitochondrial genome annotation. Mol. Phylogenet. Evol. 69, 313–319. https://doi.org/10.1016/j.ympev.2012.08.023.

Bolger, A.M., Lohse, M., Usadel, B., 2014. Trimmomatic: a flexible trimmer for Illumina sequence data. Bioinformatics 30, 2114–2120. https://doi.org/10.1093/bioinformatics/btu170.

Bouckaert, R., 2010. DensiTree: making sense of sets of phylogenetic trees. Bioinformatics 26, 1372–1373. https://doi.org/10.1093/bioinformatics/btq110.

Bouckaert, R., Vaughan, T.G., Barido-Sottani, J., Duchene, S., Fourment, M., Gavryushkina, A., Heled, J., Jones, G., Kuhnert, D., De Maio, N., Matschiner, M., Mendes, F.K., Muller, N.F., Ogilvie, H.A., du Plessis, L., Popinga, A., Rambaut, A., Rasmussen, D., Siveroni, I., Suchard, M.A., Wu, C.H., Xie, D., Zhang, C., Stadler, T., Drummond, A.J., 2019. BEAST 2.5: An advanced software platform for Bayesian evolutionary analysis. PLoS Comput. Biol. 15, e1006650. https://doi.org/10.1371/journal.pcbi.1006650.

Bravo, G.A., Remsen Jr., J.V., Brumfield, R.T., 2014. Adaptive processes drive ecomorphological convergent evolution in antwrens (Thamnophilidae). Evolution 68, 2757–2774. https://doi.org/10.1111/evo.12506.

Brumfield, R.T., 2005. Mitochondrial variation in Bolivian populations of the Variable Antshrike (*Thamnophilus caerulescens*). Auk 122, 414–432.

Brumfield, R.T., Tello, J.G., Cheviron, Z.A., Carling, M.D., Crochet, N., Rosenberg, K.V., 2007. Phylogenetic conservatism and antiquity of a tropical specialization: army-ant-following in the typical antbirds (Thamnophilidae). Mol. Phylogenet. Evol. 45, 1–13. https://doi.org/10.1016/j.ympev.2007.07.019.

Bryant, D., Bouckaert, R., Felsenstein, J., Rosenberg, N.A., RoyChoudhury, A., 2012. Inferring species trees directly from biallelic genetic markers: bypassing gene trees in a full coalescent analysis. Mol. Biol. Evol. 29, 1917–1932. https://doi.org/10.1093/molbev/mss086.

Capparella, A.P., 1991. Neotropical avian diversity and riverine barriers. Acta Congressus Internationalis Ornithologici 20, 307–316.

Cheng, H., Sinha, A., Cruz, F.W., Wang, X., Edwards, R.L., d'Horta, F.M., Ribas, C.C., Vuille, M., Stott, L.D., Auler, A.S., 2013. Climate change patterns in Amazonia and biodiversity. Nat. Commun. 4, 1411. https://doi.org/10.1038/ncomms2415.

Cheng, K.O., Hutter, C.R., Wood Jr., P.L., Grismer, L.L., Brown, R.M., 2020. Larger, unfiltered datasets are more effective at resolving phylogenetic conflict: Introns, exons, and UCEs resolve ambiguities in Golden-backed frogs (Anura: Ranidae; genus *Hylarana*). Mol. Phylogenet. Evol. 151, 106899. https://doi.org/10.1016/j.ympev.2020.106899.

Chevreux, B., Wetter, T., Suhai, S., 1999. Genome sequence assembly using trace signals and additional sequence information. Comput. Sci. Biol.: Proc. German Conf. Bioinform. 99, 45–56.

Clements, J.F., Schulenberg, T.S., Iliff, M.J., Billerman, S.M., Fredericks, T.A., Sullivan, B. L., Wood, C.L., 2019. The eBird/Clements Checklist of Birds of the World: v2019. Downloaded from https://www.birds.cornell.edu/clementschecklist/download/.

Cory, C.B., Hellmayr, C.E., 1924. Catalogue of birds of the Americas and the adjacent islands. Part III. Pteroptochidae, Conopophagidae, Formicariidae. Field Museum of Natural History Zoological Series Vol. XIII.

Danecek, P., Auton, A., Abecasis, G., Albers, C.A., Banks, E., DePristo, M.A., Handsaker, R. E., Lunter, G., Marth, G.T., Sherry, S.T., McVean, G., Durbin, R., Group, G.P.A., 2011. The variant call format and VCFtools. Bioinformatics 27, 2156–2158. http://doi.org/10.1093/bioinformatics/btr330.

Dickinson, E.C., Christidis, L.E., 2014. The Howard & Moore complete checklist of the birds of the world, 4th Edition. Aves Press, Eastbourne, U.K.

Earl, D.A., vonHoldt, B.M., 2012. STRUCTURE HARVESTER: a website and program for visualizing STRUCTURE output and implementing the Evanno method. Conserv. Genet. Resour. 4, 359–361.

Eckert, A.J., Carstens, B.C., 2008. Does gene flow destroy phylogenetic signal? The performance of three methods for estimating species phylogenies in the presence of gene flow. Mol. Phylogenet. Evol. 49, 832–842. https://doi.org/10.1016/j.ympev.2008.09.008.

Evanno, G., Regnaut, S., Goudet, J., 2005. Detecting the number of clusters of individuals using the software STRUCTURE: a simulation study. Mol. Ecol. 14, 2611–2620. https://doi.org/10.1111/j.1365-294X.2005.02553.x.

Faircloth, B.C., 2013. illumiprocessor: a trimmomatic wrapper for parallel adapter and quality trimming. 10.6079/J9ILL.

Faircloth, B.C., 2015. PHYLUCE is a software package for the analysis of conserved genomic loci. Bioinformatics 32, 786–788. https://doi.org/10.1093/bioinformatics/btv646.

Faircloth, B.C., McCormack, J.E., Crawford, N.G., Harvey, M.G., Brumfield, R.T., Glenn, T.C., 2012. Ultraconserved elements anchor thousands of genetic markers spanning multiple evolutionary timescales. Syst. Biol. 61, 717–726. https://doi.org/10.1093/sysbio/sys004.

Fick, S.E., Hijmans, R.J., 2017. Worldclim 2: New 1-km spatial resolution climate surfaces for global land areas. Int. J. Climatol.

Hackett, S.J., Rosenberg, K.V., 1990. Comparison of phenotypic and genetic differentiation in South American Antwrens (Formicariidae). Auk 107, 473–489.

Hahn, C., Bachmann, L., Chevreux, B., 2013. Reconstructing mitochondrial genomes directly from genomic next-generation sequencing reads—a baiting and iterative mapping approach. Nucleic Acids Res. 41, e129. https://doi.org/10.1093/nar/gkt371.

Harris, R.B., Alström, P., Ödeen, A., Leache, A.D., 2018. Discordance between genomic divergence and phenotypic variation in a rapidly evolving avian genus (*Motacilla*). Mol. Phylogenet. Evol. 120, 183–195.

Harvey, M.G., Bravo, G.A., Claramunt, S., Cuervo, A.M., Derryberry, G.E., Battilana, J., Seeholzer, G.F., Shearer, M.J., Faircloth, B.C., Edwards, S.V., Pérez-Emán, J.L., Moyle, R.G., Sheldon, F.H., Aleixo, A., Smith, B.T., Chesser, R.T., Silveira, L.F., Cracraft, J., Brumfield, R.T., Derryberry, E.P., in review. The evolution of a tropical biodiversity hotspot.

Harvey, M.G., Smith, B.T., Glenn, T.C., Faircloth, B.C., Brumfield, R.T., 2016. Sequence capture versus restriction site associated DNA sequencing for shallow systematics. Syst. Biol. 65, 910–924. https://doi.org/10.1093/sysbio/syw036.

del Hoyo, J., Elliott, A., Sargatal, J., Christie, D.A., de Juana, E., (Eds.) 2019. Handbook of the Birds of the World Alive. Lynx Edicions, Barcelona (retrieved from http://www.hbw.com/ on 13/11/2019).

Irestedt, M., Fjeldsa, J., Nylander, J.A., Ericson, P.G., 2004. Phylogenetic relationships of typical antbirds (Thamnophilidae) and test of incongruence based on Bayes factors. BMC Evol. Biol. 4, 23. https://doi.org/10.1186/1471-2148-4-23.

Isler, M.L., Isler, P.R., Whitney, B.M., 1998. Use of vocalizations to establish species limits in antbirds (Passeriformes: Thamnophilidae). Auk 115, 577–590. https://doi.org/10.2307/4089407.

Isler, M.L., Rodrigues Lacerda, D., Isler, P.R., Hackett, S.J., Rosenberg, K.V., Brumfield, R.T., 2006. *Epinecrophylla*, a new genus of antwrens (Aves: Passeriformes: Thamnophilidae). Proc. Biol. Soc. Wash 119, 522–527.

Isler, M.L., Whitney, B.M., 2018. Reevaluation of the taxonomic positions of members of the *Epinecrophylla fjeldsaai* (Aves: Passeriformes: Thamnophilidae) antwren complex including *E. fjeldsaai* based on vocalizations. Wilson J. Ornithol. 130, 908–914.

Jombart, T., Ahmed, I., 2011. adegenet 1.3-1: new tools for the analysis of genome-wide SNP data. Bioinformatics 27, 3070–3071. https://doi.org/10.1093/bioinformatics/btr521.

Jombart, T., Devillard, S., Balloux, F., 2010. Discriminant analysis of principal components: a new method for the analysis of genetically structured populations. BMC Genet. 11, 94. https://doi.org/10.1186/1471-2156-11-94.

Katoh, K., Misawa, K., Kuma, K., Miyata, T., 2002. MAFFT: a novel method for rapid multiple sequence alignment based on fast Fourier transform. Nucl. Acids Res. 30, 3059–3066. https://doi.org/10.1093/nar/gkf436.

Katoh, K., Standley, D.M., 2013. MAFFT multiple sequence alignment software version 7: improvements in performance and usability. Mol. Biol. Evol. 30, 772–780. https://doi.org/10.1093/molbev/mst010.

Krabbe, N., Isler, M.L., Isler, P.R., Whitney, B.M., Alvarez A., J., Greenfield, P.J., 1999. A new species in the Myrmotherula haematonota superspecies (Aves; Thamnophilidae) from the western Amazonian lowlands of Ecuador and Peru. The Wilson Bulletin 111, 157–165.

Lanfear, R., Calcott, B., Ho, S.Y.W., Guindon, S., 2012. PartitionFinder: combined selection of partitioning schemes and substitution models for phylogenetic analyses. Mol. Biol. Evol. 29, 1695–1701. https://doi.org/10.1093/molbev/mss020.

Li, H., Durbin, R., 2009. Fast and accurate short read alignment with Burrows-Wheeler transform. Bioinformatics 25, 1754–1760. https://doi.org/10.1093/bioinformatics/btp324.

Li, H., Handsaker, B., Wysoker, A., Fennell, T., Ruan, J., Homer, N., Marth, G., Abecasis, G., Durbin, R., Subgroup, G.P.D.P., 2009. The Sequence Alignment/Map format and SAMtools. Bioinformatics 25, 2078–2079. https://doi.org/10.1093/bioinformatics/btp352.

Mayr, E., 1942. Systematics and the origin of species. Columbia University Press, New York.

Mayr, E., 1996. What is a species, and what is not? Phil. Sci. 63, 262–277.

McKenna, A., Hanna, M., Banks, E., Sivachenko, A., Cibulskis, K., Kernytsky, A., Garimella, K., Altshuler, D., Gabriel, S., Daly, M., DePristo, M.A., 2010. The Genome Analysis Toolkit: a MapReduce framework for analyzing next-generation DNA sequencing data. Genome Res. 20, 1297–1303. https://doi.org/10.1101/gr.107524.110.

Meirmans, P.G., 2015. Seven common mistakes in population genetics and how to avoid them. Mol. Ecol. 24, 3223–3231.

Meyer de Schauensee, R., 1970. A guide to the birds of South America. Livingston Publishing Company, Wynnewood, Pennsylvania.
Musher, L.J., Cracraft, J., 2018. Phylogenomics and species delimitation of a complex radiation of Neotropical suboscine birds (*Pachyramphus*). Mol. Phylogenet. Evol. 118, 204–221. https://doi.org/10.1016/j.ympev.2017.09.013.
Parker III, T.A., Remsen Jr., J.V., 1987. Fifty-two Amazonian bird species new to Bolivia. Bull. B.O.C. 107, 94–107.
von Pelzeln, A., Natterer, J., 1871. Zur ornithologie Brasiliens: resultate von Johann Natterers reisen in den jahren 1817 bis 1835. A. Pichler's Witwe & Sohn, Wien.
Peters, J.L., 1951. Check-list of birds of the world, vol. 7 Museum of Comparative Zoölogy, Cambridge, Massachusetts.
Pritchard, J.K., Stephens, M., Donnelly, P., 2000. Inference of population structure using multilocus genotype data. Genetics 155, 945–959.
de Queiroz, K., 2007. Species concepts and species delimitation. Syst. Biol. 56, 879–886. https://doi.org/10.1080/10635150701701083.
Rambaut, A., 2009. FigTree v1.4.4. Available via http://tree.bio.ed.ac.uk/software/figtree/. Accessed 25/11/2018.
Rambaut, A., Drummond, A.J., Xie, D., Baele, G., Suchard, M.A., 2018. Posterior summarization in Bayesian phylogenetics using Tracer 1.7. Syst. Biol. 67, 901–904. https://doi.org/10.1093/sysbio/syy032.
Ratnasingham, S., Hebert, P.D.N., 2007. BOLD: The Barcode of Life Data System (http://www.barcodinglife.org). Mol. Ecol. Notes 7, 355-364. https://doi.org/10.1111/j.1471-8286.2007.01678.x.
Remsen Jr., J.V., Areta, J.I., Bonaccorso, E., Claramunt, S., Jaramillo, A., Pacheco, J.F., Ribas, C., Robbins, M.B., Stiles, F.G., Stotz, D.F., Zimmer, K.J., 2019. A classification of the bird species of South America. Am. Ornitholog. Soc. http://www.museum.lsu.edu/~Remsen/SACCBaseline.htm.
Remsen Jr., J.V., Parker III, T.A., 1984. Arboreal dead-leaf searching birds of the Neotropics. The Condor 86, 36–41.
Ridgely, R.S., Tudor, G., 1994. The birds of South America Vol II University of Texas Press, Austin, Texas, The suboscine passerines.
Rosenberg, K.V., 1997. Ecology of dead-leaf foraging specialists and their contribution to Amazonian bird diversity. Ornithological Monographs No. 48, Studies in Neotropical Ornithology honoring Ted Parker, 673–700.
Salaman, P.G.W., Stiles, F.G., Isabel Bohórquez, C., Álvarez-R., M., María Umaña, A., Donegan, T.M., Cuervo, A.M., 2002. New and noteworthy bird records from the east slope of the Andes of Colombia. Caldasia 24, 157–189.
Schulenberg, T.S., Stotz, D.F., Lane, D.F., O'Neill, J.P., Parker, T.A., III., 2007. Birds of Peru. Princeton University Press, Princeton, New Jersey.
Smith, S.A., O'Meara, B.C., 2012. treePL: divergence time estimation using penalized likelihood for large phylogenies. Bioinformatics 28, 2689–2690.
Sousa-Neves, T., Aleixo, A., Sequeira, F., 2013. Cryptic patterns of diversification of a widespread Amazonian woodcreeper species complex (Aves: Dendrocolaptidae) inferred from multilocus phylogenetic analysis: implications for historical biogeography and taxonomy. Mol. Phylogenet. Evol. 68, 410–424.
Stamatakis, A., 2014. RAxML version 8: a tool for phylogenetic analysis and post-analysis of large phylogenies. Bioinformatics 30, 1312–1313. https://doi.org/10.1093/bioinformatics/btu033.
Swofford, D.L., 1999. Phylogenetic Analysis Using Parsimony, PAUP* 4.0, b166. Sinauer Associates, Boston, Massachusetts.
Tan, H.Z., Ng, E.Y.X., Tang, Q., Allport, G.A., Jansen, J., Tomkovich, P.S., Rheindt, F.E., 2019. Population genomics of two congeneric Palaearctic shorebirds reveals differential impacts of Quaternary climate oscillations across habitats types. Sci. Rep. 9, 18172. https://doi.org/10.1038/s41598-019-54715-9.
Todd, W.E.C., 1927. New gnateaters and antbirds from tropical America, with a revision of the genus *Myrmeciza* and its allies. Proc. Biol. Soc. Washington 40, 149–177.
Wallace, A.R., 1854. On the monkeys of the Amazon. J. Nat. History Ser. 2 (14), 451–454. https://doi.org/10.1080/037454809494374.
Weir, B.S., Cockerham, C.C., 1984. Estimating F-statistics for the analysis of population structure. Evolution 38, 1358–1370.
Weir, J.T., Schluter, D., 2008. Calibrating the avian molecular clock. Mol. Ecol. 17, 2321–2328.
Whitney, B.M., 1994. Behavior, vocalizations, and possible relationships of four *Myrmotherula* antwrens (Formicariidae) from eastern Ecuador. Auk 111, 469–475.
Whitney, B.M., Isler, M.L., Bravo, G.A., Aristizábal, N., Schunck, F., Fábio Silveira, L., de Q. Piacentini, V., 2013. A new species of Epinecrophylla antwren from the Aripuanã-Machado interfluvium in central Amazonian Brazil with revision of the "stipple-throated antwren" complex. Handbook of the Birds of the World, original scientific descriptions, 263–267.
Wiley, R.H., 1971. Cooperative roles in mixed flocks of antwrens (Formicariidae). Auk 88, 881–892.
Zarza, E., Faircloth, B.C., Tsai, W.L., Bryson Jr., R.W., Klicka, J., McCormack, J.E., 2016. Hidden histories of gene flow in highland birds revealed with genomic markers. Mol. Ecol. 25, 5144–5157. https://doi.org/10.1111/mec.13813.
Zimmer, J.T., 1932a. Studies of Peruvian Birds. III. The genus *Myrmotherula* in Peru, with notes on extralimital forms. Part 1. Am. Mus. Novit. 523, 1–19.
Zimmer, J.T., 1932b. Studies of Peruvian Birds. IV. The genus *Myrmotherula* in Peru, with notes on extralimital forms. Part 2. Am. Mus. Novit. 524, 1–16.
Zimmer, K.J., Isler, M.L., 2003. Family Thamnophilidae (typical antbirds). In: del Hoyo, J., Elliott, A., Christie, D.A. (Eds.), Handbook of the Birds of the World. Lynx Edicions, Barcelona, pp. 448–681.
Zucker, M.R., Harvey, M.G., Oswald, J.A., Cuervo, A., Derryberry, E., Brumfield, R.T., 2016. The Mouse-colored Tyrannulet (*Phaeomyias murina*) is a species complex that includes the Cocos Flycatcher (*Nesotriccus ridgwayi*), an island form that underwent a population bottleneck. Mol. Phylogenet. Evol. 101, 294–302. https://doi.org/10.1016/j.ympev.2016.04.031.